STATOLITH DEVELOPMENT AND AGE DETERMINATION IN THE OMMASTREPHID SQUID ILLEX ILLECEBROSUS (LESUEUR, 1821)

CENTRE FOR NEWFOUNDLAND STUDIES

TOTAL OF 10 PAGES ONLY
MAY BE XEROXED

(Without Author's Permission)

CLAUDE CONRAD MORRIS

DEC 6 1985
MEMORIAL UNIVERSITY
OF NEWFOUNDLAND

CANADIAN THESES ON MICROFICHE

I.S.B.N.

THESES CANADIENNES SUR MICROFICHE

National Library of Canada
Collections Development Branch

Canadian Theses on
Microfiche Service

Ottawa, Canada
K1A 0N4

Bibliothèque nationale du Canada
Direction du développement des collections

Service des thèses canadiennes
sur microfiche

NOTICE

The quality of this microfiche is heavily dependent upon the quality of the original thesis submitted for microfilming. Every effort has been made to ensure the highest quality of reproduction possible.

If pages are missing, contact the university which granted the degree.

Some pages may have indistinct print especially if the original pages were typed with a poor typewriter ribbon or if the university sent us a poor photocopy.

Previously copyrighted materials (journal articles, published tests, etc.) are not filmed.

Reproduction in full or in part of this film is governed by the Canadian Copyright Act, R.S.C. 1970, c. C-30. Please read the authorization forms which accompany this thesis.

THIS DISSERTATION
HAS BEEN MICROFILMED
EXACTLY AS RECEIVED

AVIS

La qualité de cette microfiche dépend grandement de la qualité de la thèse soumise au microfilmage. Nous avons tout fait pour assurer une qualité supérieure de reproduction.

S'il manque des pages, veuillez communiquer avec l'université qui a conféré le grade.

La qualité d'impression de certaines pages peut laisser à désirer, surtout si les pages originales ont été dactylographiées à l'aide d'un ruban usé ou si l'université nous a fait parvenir une photocopie de mauvaise qualité.

Les documents qui font déjà l'objet d'un droit d'auteur (articles de revue, examens publiés, etc.) ne sont pas microfilmés.

La reproduction, même partielle, de ce microfilm est soumise à la Loi canadienne sur le droit d'auteur, SRC 1970, c. C-30. Veuillez prendre connaissance des formules d'autorisation qui accompagnent cette thèse.

LA THÈSE A ÉTÉ
MICROFILMÉE TELLE QUE
NOUS L'AVONS REÇUE

NL-339 (r. 82/08)

Canada

STATOLITH DEVELOPMENT AND AGE DETERMINATION IN THE OMMASTREPHID SQUID *ILLEX ILLECEBROSUS* (LESUEUR, 1821)

by

© Claude Conrad Morris, B.Sc. (Hons.)

A Thesis submitted to the School of Graduate Studies
in partial fulfillment of the requirements
for the degree of
Master of Science

Department of Biology
Memorial University of Newfoundland
March 1983

St. John's Newfoundland

"Fortunate, indeed, who ... holds a just balance between what he can acquire and what he can use, be it great or small."

Peter Mere Latham (1789-1875)
- Collected Works -

ABSTRACT

The first complete developmental series of a cephalopod statolith with its various structures is described. A new method involving a tracing for viewing, counting and recording growth increments in invertebrate statoliths and vertebrate otoliths is detailed and used to determine a daily rate of increment formation in statoliths of young Illex illecebrosus. The number of increments increases as a function of statolith length, as a function of dorsal mantle length (DML), and also increases over time. Statolith length increases as a function of DML and also increases over time.

The larval condition is shown to progress past the rhynchoteuthion (7.5-8.5 mm DML) to 50-70 mm DML, based on a change in growth constant and retention of larval characteristics including the shape of the statolith.

Statolith length is a more accurate and precise indicator of age of the animal than is the number of growth increments.

Note on Orientation

The longitudinal embryonic body axis of cephalopods corresponds to that of other molluscs, although the functional axes of the adults do not.

During the early development of the molluscan embryo the body axes correspond to those demonstrated in annelids. As the embryo develops, however, a secondary body axis forms in the dorso-ventral plane. It is in a direction which is oblique and almost perpendicular to the longitudinal embryonic primary axis (Portmann, 1960). The mantle forms along the dorsal position of this secondary axis and the foot more ventrally. Thus, the secondary axis defines the functional dorsum and ventrum of individuals of all molluscan classes except the cephalopods.

Cephalopods present a special case in which the normal functional posture of the animal requires a turning of the body in the dorso-ventral plane, with the result that the secondary axis is approximately parallel to the original position of the primary axis. Therefore, the foot is now in an anterior position with respect to the original primary axis. Consequently, the functional anterior of the cephalopod corresponds to the ventrum of other molluscs and the functional dorsum corresponds to the embryonic anterior.

Unless specified, all directions and orientation used in this work refer to the functional axes, not the embryonic, of the cephalopod body plan.

Note on Nomenclature

In some references to the cephalopod statocyst, it is not entirely clear as to whether the word "statocyst" refers to the cavity itself, the sensory structures, or both. This problem is further compounded in the Octopoda where the sensory organs lie on the inner surface of an epithelial sac which is separated from the surrounding cartilage by a "perilymphatic space".

To avoid such possible ambiguity, I refer to the combined maculae, statoliths, cristae, anticristae and cupulae as the "static organs", to the epithelial sac exclusive of the static organs as the "static sac" and to the cavity within the static sac as the "statocoel" which is filled with a fluid, the "statolymph". In the Octopoda, the space between the static sac and the surrounding cephalic cartilage remains as the "perilymphatic space" and the fluid which it contains remains as the "perilymph" (as labelled originally by Young, 1960).

ACKNOWLEDGEMENTS

I would like to express appreciation to my supervisory committee, Dr. V. C. Barber and Dr. D. H. Steele, for their very constructive comments and advice, and particularly to my immediate Supervisor, Dr. F. A. Aldrich who initially generated my interest in the invertebrates, particularly the cephalopods, through his lectures and contagious enthusiasm.

Thanks are also due Mr. E. Sandeman and Mr. Earl Dawe of Fisheries and Oceans for arranging passage and specimen collection on the M.V. GADUS (trip 47) and to the scientific staff and crew for their hospitality.

To Mr. Kent Gilkinson who provided the computer program for the growth curve and to Mr. David Methven with whom I traded ideas and information (both graduate students at Memorial University of Newfoundland), I owe much gratitude.

Thanks are also due to Dr. J. Evans of Biology for help with increment interpretation, Dr. B. Paton of the Faculty of Medicine for technical help, to Dr. S. Reddy of the laser research group of the Department of Physics for the use of the mirror employed in this study, to Dr. M. Maguire for applying his dental equipment to such unusual uses, to Ms. Carolyn Emerson for her assistance in arranging for the Department of Biology scanning electron microscope and related facilities, and to Ms. Beverley Badcock, Clinical Clerk, for encouragement and the extra help when the work became tedious.

Lastly, but certainly not least, I must express immense gratitude to Ms. Lillian Sullivan for her fine typing skills and the final preparation of this thesis, and to Mrs. Margaret Radford whose experience, guidance and patience conquered the foils of the I.B.M. word processor.

TABLE OF CONTENTS

LIST OF TABLES

LIST OF FIGURES

GLOSSARY

Angular Acceleration - Accelerative forces associated with directional change in velocity.

Crista - A ridge of ciliated sensory epithelial cells found in the statocyst of cephalopods.

Cupula - A sail-like structure surmounting the crista of cephalopod statocysts.

Growth Increment - A periodic discontinuation detectable on a growing structure and consisting of one light (Hyaline) lamella and the following dark (Opaque) lamella.

Growth Ring - The opaque lamella of a growth increment.

Hyaline Lamella - The light lamella of a growth increment.

Kernel - The inner hyaline portion of the nucleus of a cephalopod statolith.

Linear Acceleration - Accelerative forces associated with unidirectional speed changes.

Macula - A plate-like aggregation of ciliated sensory epithelial cells.

Nucleus - The central portion of a cephalopod statolith consisting of the hyaline central kernel and the first opaque lamella surrounding the kernel.

Opaque Lamella - The opaque lamella of a growth increment. See Growth Ring.

Otolith - A solid concretion of crystals of calcium salt found in the vestibular apparatus of vertebrates and serving to detect linear acceleration and, to some extent, vibrations.

Perilymph - A fluid filling a space (perilymphatic space) between the static sac and the cartilage in the skull of octopods.

Sabbatical Periodicity - A periodicity based on interruptions occuring with a frequency of one in seven or multiple(s) of seven.

Static Organs - The structures of the statocyst involved in spatial and accelerative detection including the maculae, cristae, anticristae, cupulae and statoliths.

Static Sac - The epithelial sac, exclusive of the static organs, found in the statocysts of cephalopods.

Statocyst - The entire sensory structures involved in the detection of spatial orientation and linear and angular accelerations of invertebrates. These include static organs, statolymph and the static sac, exclusive of the static nerve.

Statolith - A solid mass, usually of calcium salt, which detects linear and angular accelerations, and is found within the statocysts of motile invertebrates.

Statolymph - The fluid found within the static sac.

Vestibular Apparatus - The organs which detect linear and angular accelerations in vertebrates.

INTRODUCTION

Statocysts are organs of equilibrium detection found in motile invertebrates. In most invertebrate groups where they are found they consist of a simple sac lined internally with ciliated sensory epithelium and contain a dense calcareous concretion known as a statolith. Movement of the animal causes a displacement of the statolith in reference to its normal position within the statocyst. This displacement is detected by the sensory epithelium; nerve impulses are then sent through the nervous system and appropriate muscular action is effected.

In cephalopods, the statocysts are a pair of complex saccular organs located ventrally within the posterior cephalic cartilage and serve in the detection of linear and angular acceleration (Figs. 1 and 2).

Comparatively little had been written on cephalopod statocysts until the past two decades. Early direct references were few and these include the works of Hamlyn-Harris (1903), Ishikawa (1924), Klein (1931) and Owsjannikow and Kowalevsky (1867). Other authors make brief references to the statocysts in works of a more general nature, such as Chun (1915) on Eledonella sp., Spirula spirula (Lamarck); and Chiroteuthis imperator (Chun); Clarke and Maul (1962) on Lepidoteuthis grimaldii (Joubin); Griffin (1897) on Nautilus pompilius L.; Isgrove (1909) on Eledone cirrosa (Lamarck); Macdonald (1855) on N. pompilius Pickford (1940) on Vampyroteuthis infernalis Chun; Thompsett (1939) on Sepia officinalis. Several authors have published on cephalopod statocysts since the description of the statocyst of Octopus vulgaris

FIGURE 1. Photograph showing posterior view of the cephalic cartilage of Illex illecebrosus (Lesueur) illustrating the location of the statocysts. (From Morris, 1980).

Legend: D - Dorsal

S - Location of Statocysts

V - Ventral

Magnification: 6X

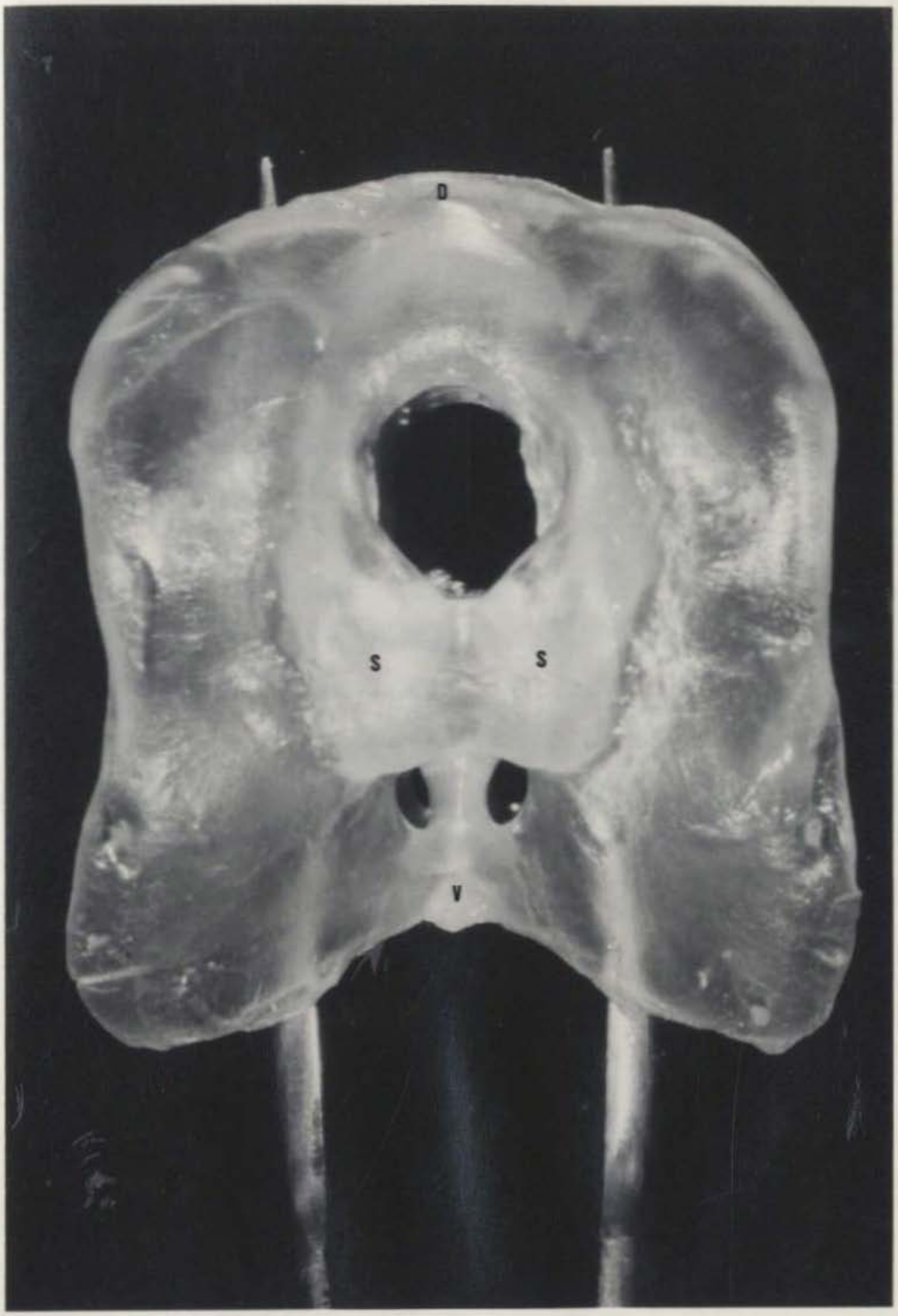
D
S
S
V

FIGURE 2. Photograph of a vertical section through the statocysts of *Illex illecebrosus* (Lesueur) showing the anterior region of the statocysts and the statoliths *in situ*. (From Morris, 1980).

Legend: AC Anticrista

D Dorsal

ST Statolith

V Ventral

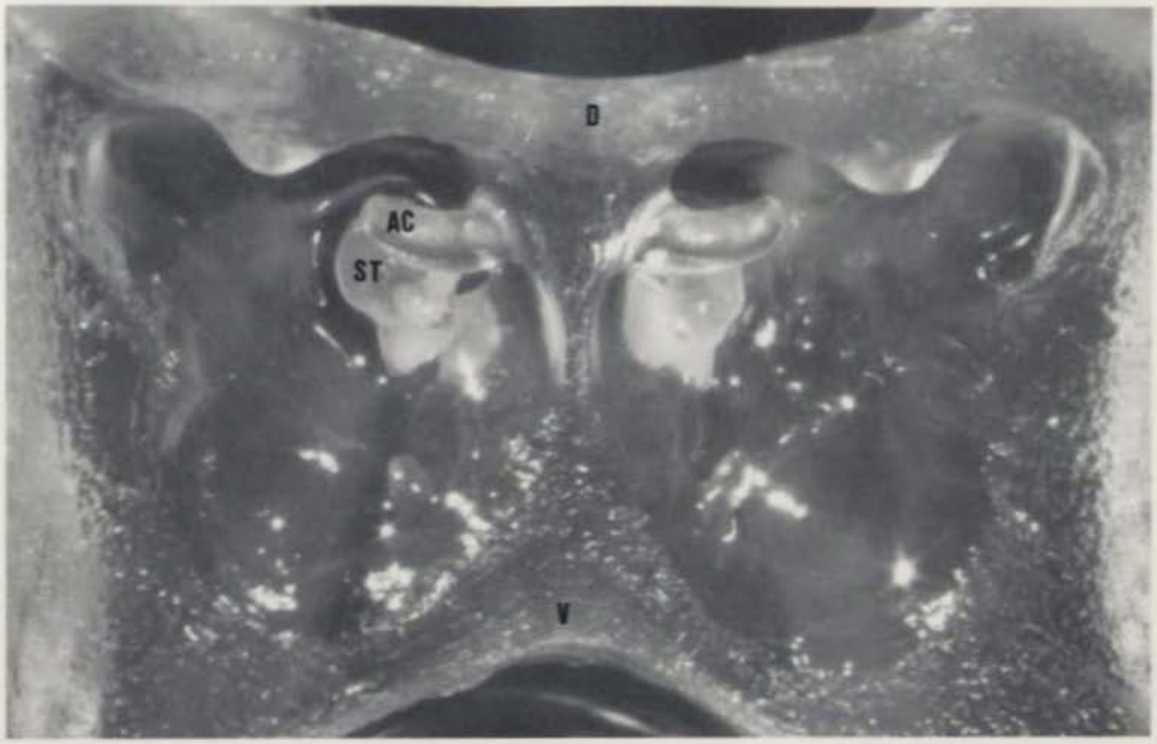

1 mm

Cuvier by Young (1960), notably Barber (1965, 1966, a and b, 1968) and Budelmann (1970, 1975, 1976, 1977, 1978, 1979).

Proprioception of the spatial orientation and movement of a cephalopod are accomplished by two mechanical systems within the statocyst (except in Nautilus which will be discussed later). These are the cristal-cupular-anticristal system and the statolith-macular system.

The first of these systems consists of a ridge, the cristal ridge, bearing interrupted rows of ciliated sensory cells interspersed with supportive cells. These ciliated areas represent the crista. This cristal ridge is roughly oriented in three axes: horizontally along the inner anterior wall of each statocyst chamber, horizontally on the exteriorad lateral wall, and vertically on the posterior wall. The crista functions in the detection of angular acceleration. The cilia are surmounted by sail-like structures called cupulae. As an animal turns, statolymph tends to lag behind the motion of the static organs in the same manner as water in a cup tends to remain motionless as the cup is rotated. The movement of the statolymph relative to the statocyst wall causes deflection of the cupula (Fig. 3). This deflection activates the underlying ciliated cells of the cristae and initiates neural transmission. Anticristae are short digitate processes projecting from the statocyst wall into the statocoel such that they restrict movement of statolymph in certain directions (Young, 1960).

Anticristae do, however, allow movement of the statolymph in the three planes perpendicular to the axes representing the orientation of the cristae. The entire functional complex of crista-cupula-anticristae

FIGURE 3. Stylized diagram to illustrate the mechanical stimulation of the sensory cilia of the crista-cupula system in a typical coleoid cephalopod.

Legend: CI Cilia of Crista

CR Crista

CU Cupula

Arrows indicate motion of the cupula caused by movement of the statolymph.

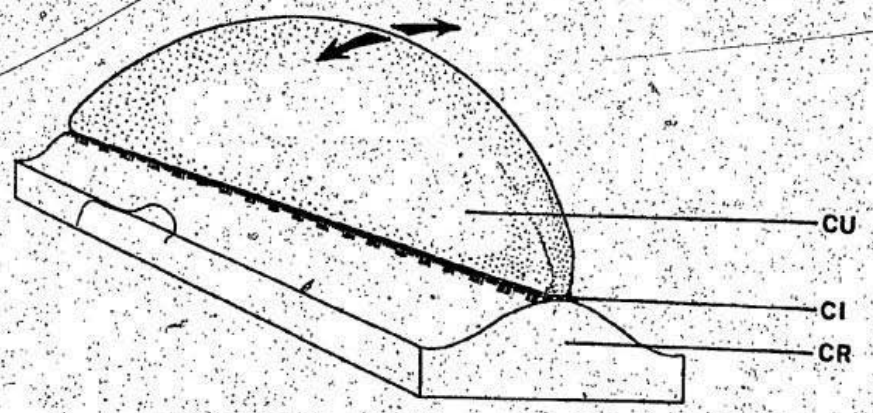
CU
CI
CR

thus forms an analog of the vertebrate vestibular apparatus (Owsjannikow and Kowalevsky, 1867; Stephens and Young, 1978, 1982).

The statolith-macular system is involved in the detection of the orientation of the animal relative to gravitational force. The statolith is situated against and loosely attached to a plate-like aggregation of ciliated sensory cells. This aggregation of cells is known as the macula and is located on the dorso-medial portion of the statocyst. As the animal moves about, the statolith tends to lag, causing it to become displaced, resulting in a shearing effect between macula and the statolith. Thus, there is initiated activation of the sensory cells of the macula (Budelmann, 1978) (Fig. 4).

It remains to discuss the statolith and associated structures as they occur in the major groups of the Class Cephalopoda, i.e., the nautiloids, the octopods and the teuthoids.

Nautiloidea

The structure of nautiloid statocysts can only be inferred from a single living genus, Nautilus. The nautiloid statocysts are simple in structure consisting of an ovoid sac evenly lined with the sensory epithelium. There is no concentration of neural receptors into maculae or cristae (Young, 1965). A duct called Kolliker's Canal connects the statocoel with the external environment (Young, 1965; Barber, 1965).

The statolith is composed of loosely aggregated spindle-shaped crystals, almost filling the statocoel. Some of these crystals extend into Kolliker's Canal (Barber, 1968; Young, 1965) (Fig. 5).

The structure of the nautiloid statolith-statocyst system is considered to be primitive when compared with those of other

FIGURE 4. Stylized diagram of a section of a coleoid cephalopod statolith and underlying macular sensory epithelium to show the mechanical stimulation of the sensory cilia of the macular cells.

Legend: CI Cilium

EM Macular Epithelium

M Organic Matrix

ST Statolith

Arrows indicate displacement of statolith.

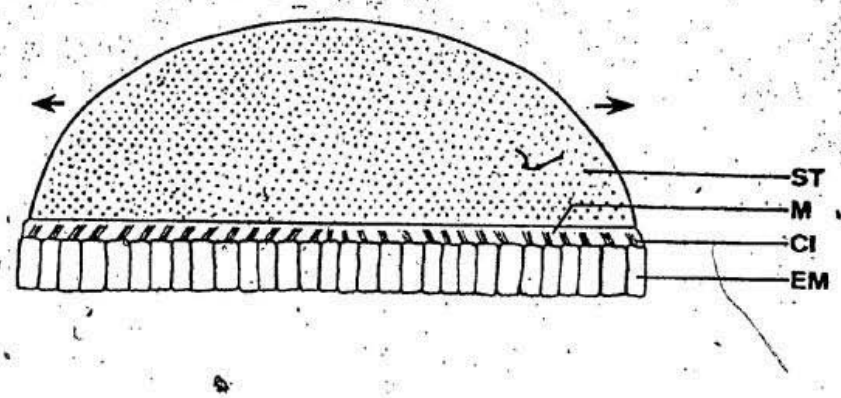
ST
M
CI
EM

FIGURE 5. Diagram of a vertical section through the statocyst of Nautilus pompilius. (L) (Re-drawn from Barber, 1968).

Legend: SN Static Nerve

K Kolliker's Canal

CC Ciliated Cell

CS Supportive Cell

CT Crystal

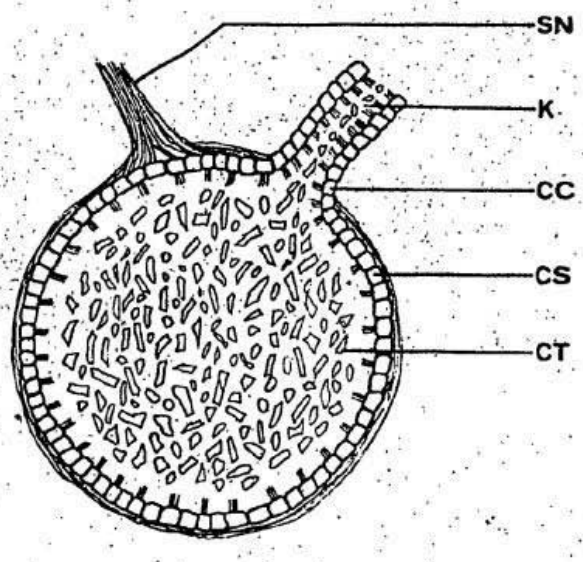
SN
K
CC
CS
CT

cephalopods, bearing a greater similarity to those of many other non-cephalopod molluscs, such as the bivalve Pecten inflexus (Buddenbrock, 1915) and the gastropod Pterotrachea coronata (Tschachotin, 1908). It is thus thought that the nautiloid statocyst represents the condition of the ancestral cephalopod equilibrium receptor.

Octopoda

The octopod statocyst is composed of an ovoid sac, herein called the static sac, suspended in an ovoid cavity within the posterior of the skull (Fig. 6). Young (1960) has referred to this sac as an endolymph sac. The cavity surrounding the sac is filled with a fluid known as perilymph, hence the name "perilymphatic space". The perilymphatic space is traversed by a network of blood vessels which supply the static sac and its contained organs. The sac is free from the surrounding cartilage except where the static nerves enter the sac in an anterior-dorsal position slightly towards the mid-line of the cephalic cartilage.

The cristal ridge is divided into three regions; (a) the crista verticalis (CV) oriented vertically on the posterior of the endolymph sac, (b) the crista longitudinalis (CL) lying horizontally along the optic lateral portion of the sac, and (c) the crista transversalis which traverses the anterior portion of the sac. Each of these cristal regions is further subdivided into three portions of approximately equal length, each bearing a cupula which projects into the interior of the static sac. There is a single hand-shaped anticrista located at the juncture between the crista verticalis and the crista longtudinalis and projecting into the fluid of the static sac.

FIGURE 6. Diagram of the statocyst of *Octopus vulgaris* Cuvier as seen from the medial aspect. (Reproduced from Young 1960) (with permission).

Legend:

AC Anticrista

BV Blood Vessel

CL Crista Longitudinalis

CU Cupula

CV Crista Verticalis

ES Endolymph Sac

K Kolliker's Canal

M Macula

NM Macular Nerve

NMC Medial Cristal Nerve

NPC Posterior Cristal Nerve

P Perilymphatic Space

PS Posterior Sac

ST Statolith

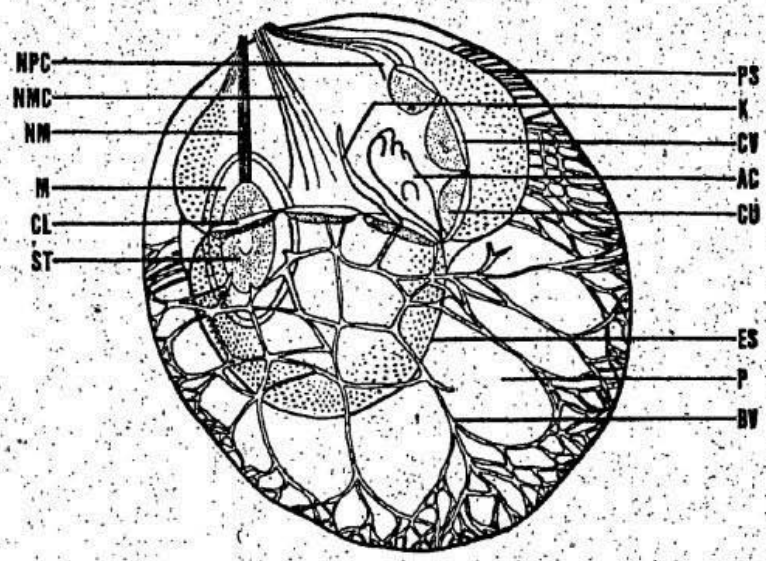
NPC
NMC
NM
M
CL
ST
PS
K
CV
AC
CU
ES
P
BV

The statolith is a low, broad cone of crystalline calcium carbonate attached to an oval macula on the medial portion of the inner wall of the anterior of the static sac (Young, 1960).

Teutholdea and Sepioidea

In the decapodous cephalopods, the static sac is applied directly to the cartilage. There is no perilymphatic space. The cristal ridge is here divided into four contiguous regions. Three of these lie horizontally in the statocyst: the crista transversalis anterior (CTA) which crosses the anterior wall of the static sac, the crista longitudinalis (CL) which traverses the optic lateral side of the static sac, and the crista transversalis posterior (CTP) which crosses part of the posterior surface of the sac. The crista verticalis (CV), the fourth region, connects by its ventral extremity to the medial end of the CTP. Each region bears a single cupula.

The number of anticristae varies. Typically, there are between five (as in Idiosepius pygmaeus Steenstrup) and thirteen (as in Thysanoteuthis rhombus Troschel), but as few as two may be found in other species, such as in Pyrgopsis (Leachia) pacifica (Issel) (Ishikawa, 1924).

There are three maculae. These are (a) the macula neglecta anterior (MNA) vertically oriented and located anteriorly on the dorsal region of the medial wall of the statocyst, (b) the macula neglecta posterior (MNP) which is horizontally oriented and located in the middle of the medial wall in a slightly anterior position, and (c) the macula statica princeps (MSP) found underneath the statolith in a dorso-medial position on the anterior statocyst wall. The MNA and MNP each bear a superficial layer of crystals of calcium carbonate.

Vampyromorpha

The single species of this order (Vampyroteuthis infernalis Chun) has a large statocyst chamber, being larger than the eyes in very young juveniles of the species (Pickford, 1940). The statocyst has the octopod characteristics of a perilymphatic space and a crista oriented in three planes. In addition, this species has the decapodous characteristic of having more than one anticrista, namely, nine in number (Barber, 1968). Vampyroteuthis has a very fragile powdery statolith (Clarke, pers. comm.). The vampyromorph statocyst is thus a structural intermediate between the Octopoda and the Teutholdea. This may represent an evolutionary link but more likely indicates an intermediate mode of life combining that of the pelagic decapodous forms and the largely benthic octopods.

Statocyst Development

Information on the early development of the statolith is very scarce. Ishikawa (1924) observed the "discoidal" statolith in newly hatched Argonauta hians (Solander) but did not give an illustration nor comment further upon it. Lipinski (1980) attempted to show the development of the statoliths of I. illecebrosus using specimens from 88 mm DML to 342 mm DML. However, of the five specimens he used, the two earliest specimens illustrated (DML 88 mm and 145 mm) were severely broken and incomplete. The third (DML 188 mm) was cracked and the fourth (DML 292 mm) was ground to show growth increments, thereby leading to a misrepresentation of morphological detail. The fifth was

not a specimen of I. illecebrosus, but rather of the genus Martialia described by Rochebrune and Mabille in 1895 of the species M. hyadesi Roch. and Mab.. Such is a poor beginning for a developmental series.

Sections of statoliths in situ from newly hatched and young squids of the species Alloteuthis subulata (DML unspecified) and Loligo pealei (DML 20 mm) have been illustrated by Stephens and Young (1982). These authors failed, however, to offer any adequate discussion of their photographs or the structural configuration therein illustrated.

Ishikawa (1924) comments that on day 7 of the embryonic development of Sepia esculenta, a small patch of cells, the statocyst anlage, appears externally on either side of the mantle anlage. By day 14 this has invaginated and narrowed at its exteriorad margin. At approximately 25 days the statocoel is formed and sealed. Simultaneously, the anlagen of the macula statica princeps and of the crista form as groups of ciliated columnar epithelial cells. A small statolith then begins to form on the dorsal region of the macula statica princeps, the entire statocyst appearing as a spheroid sac.

During the fifth week, five of the eleven anticristae form and the maculae become identical to those in the adult. Presumably, although Ishikawa does not state it, the cupulae are formed on the cristal sections at, or immediately prior to, this same time. Static nerves are also visible at this stage. Thus, as we could expect, the sepioid statocyst is fully equipped to function upon hatching.

Ishikawa further comments that the development of the statocyst in the pelagic octopods of the genus Argonauta is similar to that of S. esculenta up to the corresponding week five of the development of the decapod, except that only a single anticrista forms in Argonauta.

Teuthoid Statoliths

Teuthoid and seploid statoliths are solid concretions of crystals of aragonite, the orthorhombic form of calcium carbonate (Clarke, 1978), in a thin matrix of protein (Radtke, 1981).

Although statolith form varies considerably among teuthoids, several structures can be recognized as common to all, or nearly all, statoliths of this group. Clarke (1978) devised a standard nomenclature for these structures and a system of measurements for the statolith as a whole. Since the teuthoid statolith form is apparently species-characteristic, and because statoliths have a greater likelihood of fossilization than other cephalopod structures, their potential in identification of prehistoric species has been recognized (Clarke and Fitch, 1975). The metrical and nominal system of statolith descriptions has been used to identify several new fossil species based on single statoliths (Clarke and Fitch, 1979). However, diverse intraspecific statolith form has been demonstrated in Symplectoteuthis oualaniensis (Lesson) by Burch (1980), and considerable intraspecific and intraindividual variation has been shown in Illex illecebrosus by Morris (1980, 1981) and several other species by Clarke and Fitch, (1979). This would cast some doubts on the validity of species descriptions based solely on one statolith.

The crystals which form the statolith are in two distinctly different arrangements (Dilly, 1976; Morris, 1980). The first of these is an irregular arrangement which is found in the wing, part of the dorsal spur, and in part of the rostrum. These areas appear opaque under a light microscope (Morris, 1980) (Fig. 7). The second pattern of arrangement involves nearly parallel orientation of the long axes of the crystals radiating from the nucleus in a similar manner as spokes of a

FIGURE 7. Posterior aspect of the statolith of *Illex illecebrosus* (Lesueur) showing visible structures and measurements used in this study.

A. Light micrograph. Notice opaque region toward median side, composed of irregularly arranged crystals. (Magnification: 65x)

B. Diagram. Dotted line indicates position of Posterior Dome Indentation. Stippled area indicates region of irregularly arranged crystals.

Legend: AR Rostral Angle
DD Dorsal Dome
FM Medial Fissure
F Foramen
LI Inferior Lobe of Lateral Dome
LR Lateral Lobe of Rostrum
LS Superior Lobe of Lateral Dome
R Rostrum
DS Dorsal Spur
W Wing

C. Diagram showing axis along which total length (AB) of a statolith was measured.

(Modified from Morris, 1980: Nomenclature as from Clarke, 1978)

A

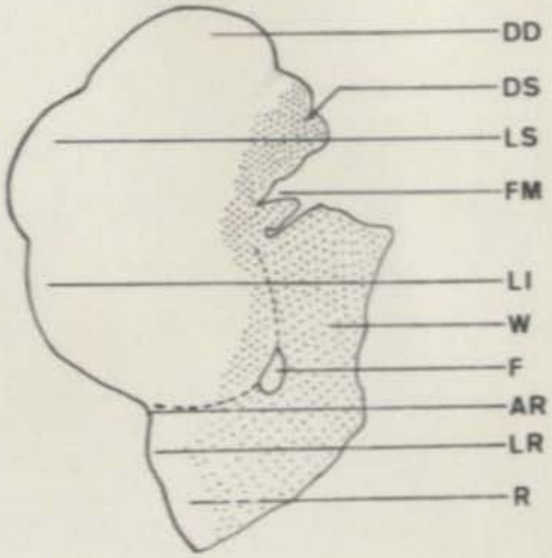

B

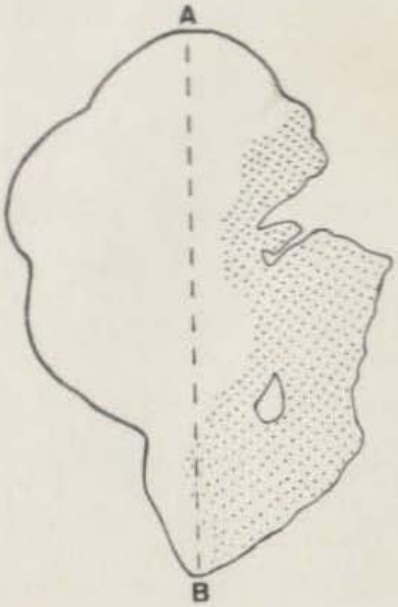

C

wheel. This arrangement is found in the dorsal and lateral domes, most of the rostrum and the central region of the statolith. These regions appear translucent under light microscopy (Morris, 1980). Growth increments, referred to usually as "growth lines", may be visible in these areas in unground specimens.

Increments

The microscopic layered patterns of alternating light and dark lamellae found in fish scales, bones and otoliths, and in the statoliths, shells and other hard structures of invertebrates, are not referred to with any standard nomenclature. They may be called "growth lines" (Dillon and Clark, 1980); "growth rings" (Hurley and Beck, 1980); or as "internal growth increments" or "microgrowth increments" (Rhoads and Lutz, 1980). A distinction between growth rings and increments has been proposed by Panella (1980) who labels each dark lamella as a ring, and an individual increment as being one light lamella plus the immediately following dark lamella. Thus, for the purposes of counting, ring and increment counting are effectively identical. However, when one considers an organism's physiological activity and the formation of such structures, a growth ring may not be properly identified with an increment. This distinction is adopted for clarity in subsequent discussion in this text. Mina (1968) has enlightened us to the fact that the lighter, or hyaline, portion of an increment is formed during periods of relatively rapid deposition of a calcium salt within an organic matrix, while darker lamellae (i.e., rings) are formed when the rate of calcium deposition slows. It has also been shown that dark lamellae are formed with the resorption of calcium from the shell of the bivalve

Mercenaria mercenaria (L.) (Gordon and Carriker, 1978). It was also demonstrated by Kristensen (1980) that the dark lamellae of increments in statoliths of Gonatus fabricii (Lichtenstein) were due to concentrations of collagenous organic material.

Although light and dark portions of increments are usually easily distinguishable, the lateral demarcation of either is not always linear or "clear cut". For example, with respect to the dark lamellar rings, they are most obvious in the central portion of their width, tending to fade into less distinct grays to either side of centre where they are, as it were, "invaded" by irregular leading edges of preceeding or subsequent light lamellae. This condition leads to difficulties in precisely measuring individual increments and/or ring widths. The width of an increment may be estimated from calculation of average widths over a given area of the increment-bearing structure. This method, however, does not apply to ring measures since they are not continuous in series as they alternate with light lamellae.

The characterization of a lamella as being either "hyaline" or "opaque" is a purely relative and qualitative designation, depending totally on the optical densities of the immediately adjacent lamellae to either side of the one being considered. Thus, a lamella of a given optical density may be considered to be "opaque" in one region of the structure under observation, yet be judged "hyaline" in some other region, depending on the optical properties of its adjacent lamellae. We must not totally discount the judgement or the ability, based on experience, of the observer.

Age Determination in Cephalopods

Several structures have been used in attempts to age cephalopods. Choe (1963) examined lamella formation on the sepions of Sepia subaculeata Sasaki, S. esculenta Hoyle, and Sepiella maindroni de Rochebrune, and found a daily periodicity for each species. However, Richard (1969) found that lamella formation in Sepia officinalis L. is temperature-dependent, reaching a daily periodicity at 30° C which was the upper limit of the water temperature obtained by Choe. The two sets of results are not considered to be in conflict (Richard, 1969).

Yagi (1960) found a nine-day periodicity of lamella formation in S. esculenta, but this is debatable since he assumes all of his captured specimens to be of the same age and subjected to the same environmental conditions (Choe, 1963).

Radulae and mandibles are not useful in age determination because they are prone to wear and breakage, as in O. vulgaris which regularly feeds on crustaceans and is known to use its radula to bore through bivalve shells. However, the crest length of the upper mandible, the length of the radular ribbon, and the weight of the octopus itself can give a rough estimate of age (Nixon, 1973). Clarke (1965) reported growth increments on beaks of the squid Moroteuthis ingens (Smith). These increments had repeating cycles of width but could only ascribe a possible periodicity of either six or twelve months to the formation of each cycle. Lu (1968) examined increments on beaks of Illex illecebrosus and correlated the numbers of increments with the DML. He further proposed that mandibles could be used in age determination. Although the diet of teuthoids consists of less abrasive material than does the diet of octopods, teuthoid mandibles can, however, be subject to considerable wear.

The correlation of the sidereal lunar month (in days) with the number of growth increments per chamber in N. pompilius was used to infer changes in lunar periodicity, based on nautiloid fossils of known ages (Kahn and Pompea, 1978). These papers caused considerable debate and are still subject to discussion and confirmation.

Young (1960) observed concentric lines within the statolith of O. vulgaris but there have been published no attempts to use this structure in the determination of the age of octopods.

Clarke (1966) detected growth increments in the Ommastrephid squids Ommastrephes caroli (Furtado), O. pteropus (Steenstrup) and Todarodes sagittatus (Lamarck) but did not find any cyclical periodicity or major fluctuations. His interpretation of these increments was limited by their small size.

Spratt (1979) identified length frequency modes and followed their seasonal progression in the squid Loligo opalescens Berry. He concluded that this species had a life span of 2.5 years. In attempting to confirm his hypothesis, Spratt examined the statoliths of L. opalescens and assumed a daily increment formation near the nucleus where the increments were closely spaced. He also ascribed monthly periodicity to increment formation in the peripheral areas where the increments appear to be wider and fewer, demonstrating a light region followed by a dark region, together representing one growth increment over a one-month period of time. Other authors have assumed these peripheral increments to be daily (Hurley and Beck, 1980; Rosenberg, Wiborg and Bech, 1981; Kristensen, 1980). However, the increments they describe are more narrow and more numerous than those described by Spratt (1979).

Kristensen (1980) showed cycles of narrow growth increments in the extranuclear areas of statoliths of Gonatus fabricii. These cycles were of alternating light and dark bands, each band consisting of several narrow dark increments, and similarly each light band consisting of several light increments. The average number of these increments per band was 13.2, indicating that the period of one cycle of increments (one light band plus one dark band) as 26.4 increments. This is closer to the number of days in a lunar synodic month (29.53 days).

Rosenberg, et al (1981) found a linear relationship between statolith growth increment counts and dorsal mantle length in the range of 15.0 to 25.0 cm for Todarodes sagittatus (Lamarck). By assuming that these increments are daily, they verified the presence of fortnightly regions (14.0 increments per region) as described independently by Kristensen (1980).

Lipinski (1978) found growth increments in statoliths from I. illecebrosus and, like Spratt, assumed daily periodicity near the nucleus and monthly periodicity in the peripheral areas. However, Hurley and Beck (1980) assumed daily periodicity throughout the statolith of I. illecebrosus, as did Lipinski (1979). A less detailed account of ageing of teuthoids than has been presented here has been given by Dawe (1981).

Positive correlations of statolith increment counts with total statolith length and dorsal mantle length were found by Lipinski (1980).

Although some of the work contained herein may be viewed as a repetition of that of Lipinski (1980), I expand the range of Lipinski's data and increased the number of data points in an effort to achieve a more satisfactory approximation of the phenomena observed. Furthermore,

It is herein attempted to establish whether the formation of growth increments on the statolith of I. illecebrosus is daily, as was assumed by Hurley, et al (1979) and Hurley and Beck (1980). If the periodicity of increment formation is either irregular or non-daily, or is based on some other time interval, it is attempted herein to establish what other parameter may be employed in an assessment of the age of I. illecebrosus with precision and reasonable accuracy.

The thesis also describes for the first time stages in the structural development of a cephalopod statolith and its several parts and features. It is true that Lipinski (1980) presented photographs of statoliths of I. illecebrosus to show development, but he failed to label the developing structures and thus trace their developmental anatomy and adult configuration.

Over the years 1979 through 1982, I have personally observed the statoliths, both right and left, of more than 400 specimens of I. illecebrosus. These cover a wide range of sizes from numerous locations around the island of Newfoundland, mainly Conception Bay. It is on such a large "data base" that I have based my analysis of the configuration of the morphological characteristics of the statolith. Some of this knowledge gained served as the basis of my Honours B.Sc. thesis (1980) and more is presented herein for the first time, especially the developmental series elucidating the ontogeny of the statolith from Primordial through Advanced Stages.

MATERIALS AND METHODS

Specimens of I. illecebrosus were captured on five different occasions during 1981 (Table I) (Fig. 8). Small juvenile specimens of dorsal mantle length (DML) of 31 mm or less were placed in glass vials with sea water and frozen. Larger specimens were put in plastic bags and preserved in like manner until examination.

Specimens in vials were thawed by exposure to room temperature. Those in plastic bags were placed inside a second plastic bag and immersed in lukewarm water to thaw.

Statolith removal was performed by placing the squid on its dorsum, lifting the funnel away from the body, and severing the tissues which attach the funnel to the head. A subsequent vertical incision immediately anterior to the liver and behind the head to the depth of the esophagus exposed the broad posterior cephalic cartilage. Removal of the tissues surrounding the cartilage exposes the two convex cartilaginous protruberances of the posterior cephalic cartilage that indicate the position of the paired statocysts. At this point, the statoliths can usually be seen through the intervening cartilage.

The statocysts were opened by raising the posterior of the head off the dissecting board and making a horizontal incision through the posterior cephalic cartilage to remove the floors of the statocyst chambers. The statoliths were separated from their maculae with fine forceps and stored in glycerine. A dissecting microscope was not required in this operation except in the cases of the smallest specimens.

TABLE I. Capture data for specimens of *Illex illecebrosus* used in the study of statoliths. All specimens were taken during the year 1981

Date of Capture (1981)	Location (Lat., Long.)	Location (General)	Gear	Depth (Meters)
Feb. 27	38° 24.7' N 56° 00.0' W	Gulf Stream	Engel Midwater Trawl	100
Mar. 4	41° 14.9' N 53° 00.0' W	Gulf Stream	Engel Midwater Trawl	100
May 25	45° 00.1' N 45° 30.0' W	Carson Canyon	Engel Midwater Trawl	500
June 20	43° 36.5' N 51° 54.8' W	Grand Banks	Engel Midwater Trawl	124
Oct. 13	47° 45.1' N 54° 01.2' W	Refinery Pier, Come By Chance	Japanese Jig Rig	10

FIGURE 8. Map of Northern Gulf Stream region and insular waters of Newfoundland, showing sites of capture of *Illex illecebrosus* (Lesueur) used in this study of statoliths.

1. Feb. 27, 1981; 10 animals at 38° 24.7'N, 56° 00.0'W, DML Range 13.5 - 29.0 mm

2. Mar. 4, 1981; 3 animals at 41° 14.9'N, 53° 00.0'W, DML Range 21.0 - 30.0 mm

3. May 25, 1981; 5 animals at 45° 00.1'N 45° 30.0'W, DML Range 109 - 118 mm

4. June 20, 1981; 52 animals at 43° 36.5'N, 51° 54.8'W, DML Range 130 - 191 mm

5. Oct. 13, 1981; 42 animals at 47° 45.1'N, 54° 01.2'W, DML Range 225 - 266 mm

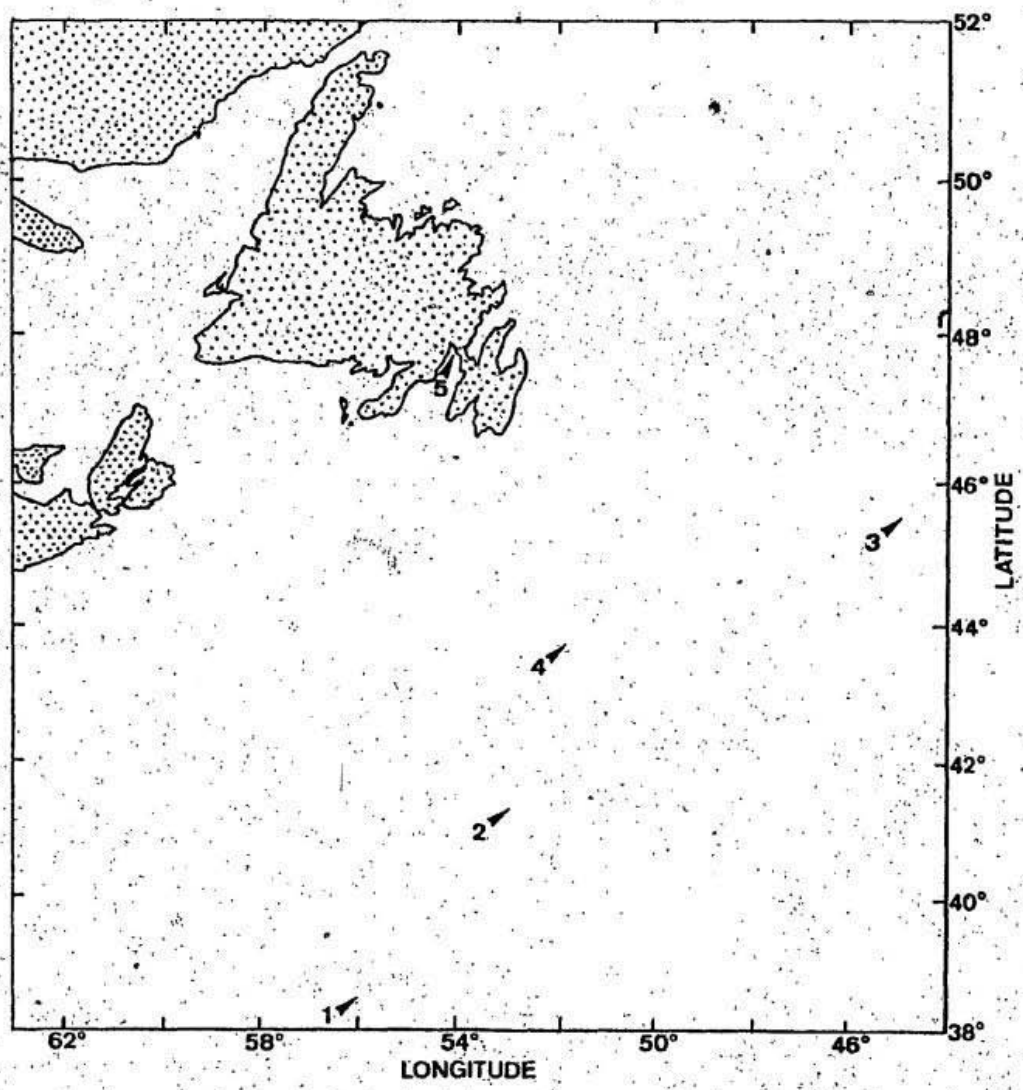
52°
50°
48°
46°
44°
42°
40°
38°
LATITUDE
62°
58°
54°
50°
46°
LONGITUDE
1
2
3
4
5

Excess tissue and organic debris adhering to the statoliths were dissected away under a microscope with any persisting debris removed by placing in 5% hypochlorite for up to three minutes. This treatment dissolved any remaining debris. The statoliths were then washed in two changes of distilled water and mounted in glycerine on a glass slide for measurement.

Measurements were taken of the maximum length of each statolith of a pair, such measurements extending from the most dorsal point of the dorsal dome to the tip of the rostrum (Fig. 7). The average value of both measurements of a given pair was taken as the datum point for that animal.

Quantification of statolith lengths was performed with a binocular Nikon microscope (Model S-Ke II) equipped with HKW 10X eyepieces and a corresponding eyepiece micrometer.

Following measurement, statoliths were placed in 95% ethanol for one minute to remove glycerine, washed in two changes of distilled water for similar periods, and placed on a glass slide to dry. Excess water was removed with Kimwipe tissues.

After drying, the statoliths were mounted in EPON 812 resin (Fisher Scientific Co., New Jersey, U.S.A.) with the concave anterior surface facing upward and the dorsal dome inclined slightly downward (Fig. 9). This latter manoeuvre allows best observation of growth increments near the free margin of the dorsal dome. This site is an area where growth increment resolution is frequently lost in improperly mounted specimens (Fig. 10).

The slides were then placed in a Fisher Senior Isotemp oven at 50° C for 8 to 12 hours until the EPON 812 was polymerized. Checking

FIGURE 9: Longitudinal section of a mounted statolith of *Illex illecebrosus* (Lesueur) prepared for grinding.

Legend: CO - Occulting Crystals

DD - Dorsal Dome

GI - Growth Increment

N - Nucleus

R - EPON 812 Resin

S - Glass Slide

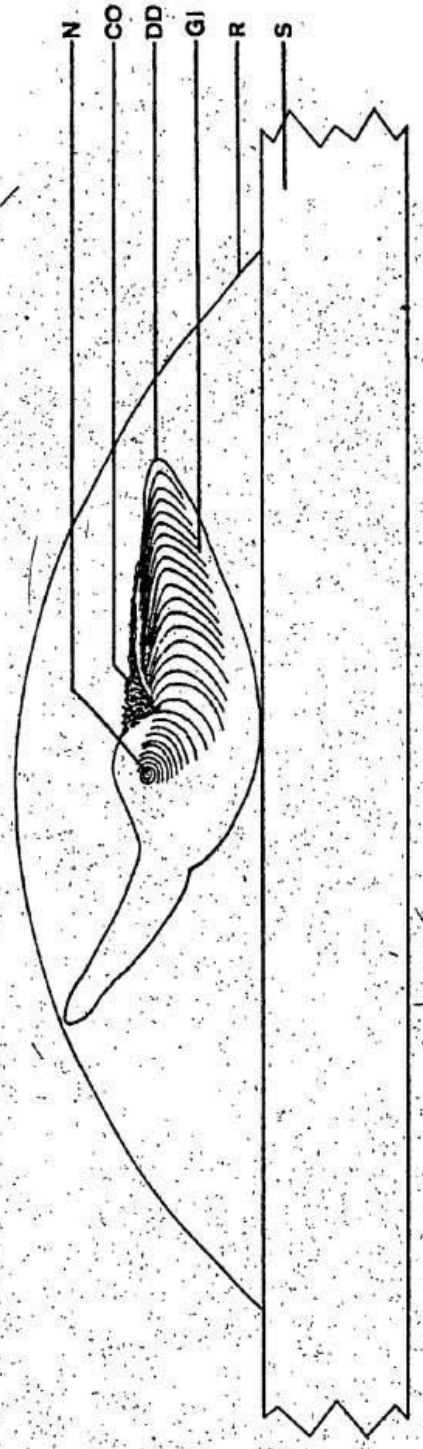
N
CO
DD
GI
R
S

FIGURE 10. Photograph of the dorsal dome region of a statolith of *Illex illecebrosus* (Lesueur) showing obliteration of increments at the periphery of the statolith caused by excessive abrasion during preparation for observation.

100 um

the slides after heating for three hours to ensure that the statoliths had not rolled from their original positions greatly improved the success rate in producing specimens with growth increments clearly visible over the range area extending from the nucleus to the free margin of the dorsal dome.

The slides were then ground against a glass plate covered with a mixture of 1200 grit carborundum powder and glycerine until the nucleus was clearly visible. Since glycerine does not evaporate as quickly as water, the rate of grinding and the "feel" of the grinding is more consistent. Tilting of the slide in different directions can help direct the abrasive effect to particular areas of the statolith as required. Constant checking of the progress of grinding is required as grinding past the depth of the nucleus obliterates the growth increments.

Following grinding, there may become apparent a second area of obscured increments located near the nucleus. Here, an area of large irregular crystals lay in a depression near the nucleus (Figs. 11 and 12). The diffractive and refractive effects of these crystals obscure the underlying increments and may render them uncountable. Attempts to remove them by prying with steel needles, grinding with ground glass needles and scraping with dental picks were unsuccessful. The use of a dental drill with the finest available bit proved to be too coarse and greatly marred the entire statolith surface.

Many, if not all, of these crystals can be removed during the main grinding process if the dorsal dome is not depressed at too steep an angle. Since failing to depress the dorsal dome obliterates the increments on it, a balance must be found between both positions. A

FIGURE 11. Diagram to show the optimum plane of grinding through a statolith of Illex illecebrosus (Lesueur) to reveal growth increments.

Legend: AB - Grinding Plane

CO - Occulting Crystals

S - Microscope Slide

FIGURE 12. Diagram to show a statolith of Illex illecebrosus (Lesueur) with growth increments not visible. Note the intersection of the grinding plane (CD) with the occulting crystals indicating that some crystals would remain after the grinding proceedure.

Legend: CD - Grinding Plane

CO - Occulting Crystals

S - Microscope Slide

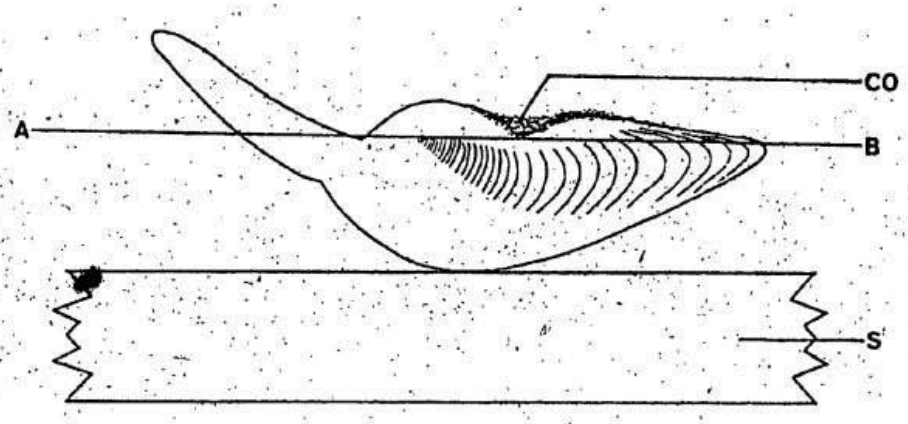
CO
A
B
S

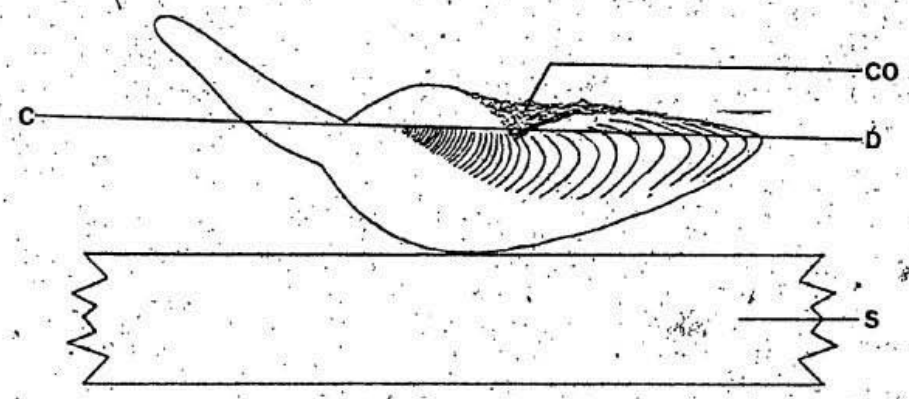
CO
C
D
S

slight downward inclination of the dorsal dome seems most useful with good results usually being obtained when depression of the dome approximated 10° below the horizontal.

The alternating light and dark growth increments on otoliths of fish and statoliths of squid have been referred to by numerous authors. They are formed by differential ratios of calcium carbonate in a proteinaceous matrix. The darker lines containing more protein (Mina, 1968) can be accented using a proteinophyllic stain. The stain used here for ground specimens was ninhydrin, buffered in phosphate at pH 6.95 and applied for two minutes with the slides bearing the specimens suspended 4 cm over boiling water (Humason, 1972). The EPON adjacent to the statolith in these preparations was counterstained with 0.1% fast green for one minute, again over boiling water. Since ninhydrin deteriorates rapidly, the slides must be viewed immediately after staining. Fast green is also proteinophyllic and because red and green are complementary colours, any protein reacting with both stains will appear dark.

With the specimen in place on the microscope stage, and looking at the stage from the side in a darkroom, movements of the stage micrometer will produce a red "halo" effect near the specimen. The intensity of the red colouration serves as a check for the freshness of the ninhydrin.

In a darkroom, a Zeiss microprojector was used to project images of the stained specimens into a 20 cm diameter aluminium surface coated mirror and reflected onto a sheet of matt surface paper of the whitest quality available to observe growth increments. The surface coating of such a mirror eliminates the double reflection due to the glass and

silvered surfaces of a typical mirror, and eliminates as well the production of false increment images. The magnification thus produced (690x) facilitated not only observation, but also the tracing of the increments directly onto the white paper while the image was thereon projected. This method was used for both unstained and stained ground statolith preparations.

Counting of the growth increments proceeded from the nucleus of the statolith toward and across the dorsal dome. This is the longest axis of growth increment formation and consequently is the axis of widest separation and best resolution of those increments. The width of an increment is represented in the width of a corresponding line drawn on paper, and the darkness of an increment by the length of the drawn line (Fig. 13). After a minimum of three complete tracings for each statolith, the numbers of lines on the tracings were counted. This procedure eliminates bias from observing the size of a statolith and unconsciously counting enough increments to correspond to the expected number for that particular size statolith.

The accepted value of the number of increments for a given statolith was the average of the two highest counts which did not differ by more than five percent. Specimens of ground statoliths of Illex illecebrosus were also prepared for observation under the scanning electron microscope (Cambridge Stereo Mk II) by dehyration in absolute ethanol, air drying, and then coating with gold in an Edwards S 150A sputter coater.

FIGURE 13. Tracing of rings observed in ground and stained specimen of statolith of Illex illecebrosus (Lesueur). The length of line representing one ring indicates relative darkness while width of same line indicates width of ring being traced.

N - Nucleus

RESULTS

A. General

Sampling sites of Illex illecebrosus were situated progressively closer to the island of Newfoundland at successive sampling dates in 1981. Increasing mean values of DML and statolith length are also evident (Table 2).

In the two earliest samples (February and March), which contained the smallest specimens, the squid exhibited several larval characteristics such as a loose saccular mantle, wide proximal aperture of the hyponome (or funnel), large eyes, and a posteriorly convex fin. Characteristically, statoliths could be removed from even the smallest specimen (13.5 mm DML) and upon microscopic examination were seen to demonstrate serial increments, as described by other authors and as described herein earlier in the introduction.

Specimens taken in June were still relatively small but were similar morphologically to the adults later taken in samples in the month of October.

B. Statolith Development

In its development, the first part of a teuthoid statolith to be formed and subsequently recognized is the kernel which is a small hyaline spheroidal area lying, in the adult animal, near the wing of the statolith. It is visible in statoliths from very young specimens (Fig. 13) and in ground statoliths from adult specimens. Growth increments in the kernel are either not detectable or are very indistinct.

As larger specimens with larger statoliths (Table 2) are taken at progressively later dates, the statolith becomes increasingly complex and passes through several distinct stages. These stages are now

TABLE 2. General population data and statolith data of specimens of *Illex illecebrosus* used in this study. All specimens were taken during the year 1981. Means and ranges given are for females only.

Date of Capture	Location (Lat., Long.)	Number Unsexable	Number Males	Number Females	Total	DML Range (mm)	DML Mean (mm)	Statolith Length (um) (Range)	Statolith Length (um) (Mean)
Feb. 27	38°24.7'W 56°00.0'W	9	-	-	9	13-29	18.6	281-442	314.9
Mar. 4	41°14.9'N 53°00.0'W	3	-	-	3	21-30	26.0	366-397	386.8
May 25	45°00.1'N 45°30.0'W	-	5	0	5	109-118	114.4	772-818	794.0
June 20	43°36.5'N 51°54.8'W	-	30	19	49	157-191	167.6	851-945	888.4
Oct. 15	47°45.1'N 54°01.2'W	-	33	15	48	229-271	249.7	1033-1139	1086.0

described and names given to the several posthuclear stages. They are: 1) Primordial, 2) Definitive, 3) Pre-Juvenile, 4) Juvenile, 5) Adult, and 6) Advanced Stages.

1) Primordial Stage

The developmental stage that follows nucleus formation (see Discussion) is a roughly tear-drop or lachrymiform structure, with the tip directed ventrally and flexed slightly anteriorly and laterally (Fig.14). This primordial stage is found in specimens of 12 to 16 mm DML. The dorsal region of this structure, the dome anlage, is the precursor of the dorsal dome and superior lateral dome. The medial curvature, after enlarging as the statolith grows, will later serve as an attachment site for the wing. The apex of the lachrymiform shape is the rostrum anlage. This stage was observed in statoliths from three squid.

2) Definitive Stage

The second stage in post-nucleus statolith development, here named the Definitive Stage, occurs in squid of approximately 30 mm DML (Fig. 15). The dorsal dome, superior lateral dome and inferior lateral dome are forming and becoming identifiable. The rostrum anlage has now developed sufficiently to be recognized as a rostrum and is in the course of altering its direction of growth, curving toward the midline of the cephalic cartilage in situ. Upon the medial aspect of the rostrum are to be seen small irregularly arranged crystals which form the anlage of the wing. Irregular crystals which effectively occult the underlying increment lines have begun to form in the dorsal region in this stage. Also developing in the dorso-medial region is the structure known as the dorsal spur. This stage was observed in statoliths from nine squid.

FIGURE 14. Primordial Stage in the development of a left statolith of *Illex illecebrosus* (Lesueur) from an unsexed specimen of 13.5 mm dorsal mantle length. (Anterior view). Specimen mounted in glycerine.

Legend: D - Dorsal
DA - Dome Anlage
N - Nucleus
MC - Medial Curvature
RA - Rostrum Anlage
V - Ventral

FIGURE 15. Definitive Stage in the development of a left statolith of *Illex illecebrosus* (Lesueur) from an unsexed specimen of 29.0 mm dorsal mantle length. (Anterior view). Specimen is mounted in glycerine.

Legend: CO - Occulting Crystals
D - Dorsal
DD - Dorsal Dome
DS - Dorsal Spur
LI - Inferior Lateral Dome
LS - Superior Lateral Dome
RO - Rostrum
V - Ventral
WA - Wing Anlage

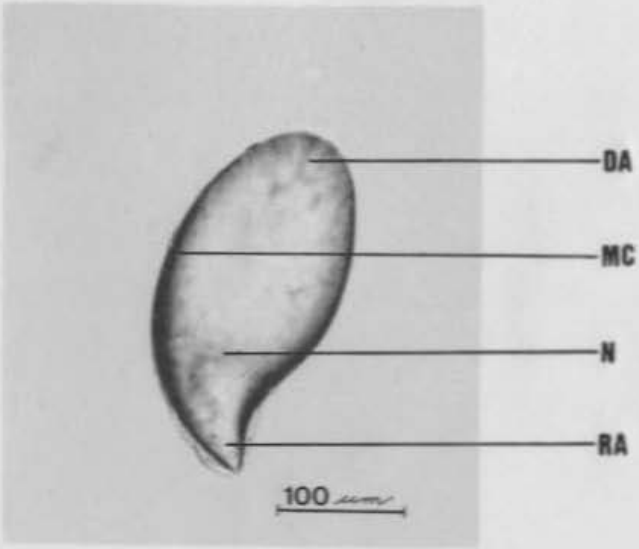
DA
MC
N
RA
100 µm

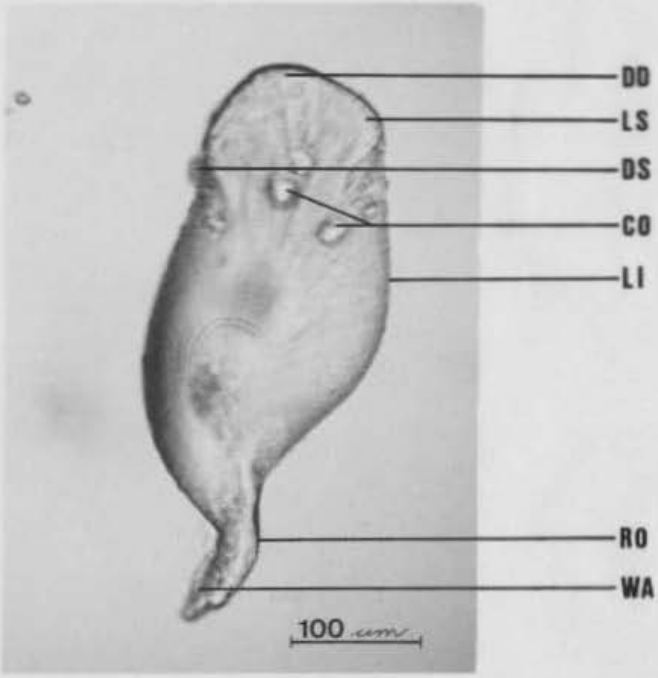
DD
LS
DS
CO
LI
RO
WA
100 µm

3) Pre-Juvenile Stage

The third stage, the Prejuvenile Stage, is not herein illustrated due to lack of specimens. However, several of its characteristics may be inferred, and for the sake of continuity I will speculate on both its appearance and its role in the developmental series here noted. The rostrum extends ventrally, and curves slightly toward the median of the animal. The wing extends medially, then turns anteriorly toward the medial curvature. The dorsal spur is distinct as are the dorsal and lateral domes. Occulting crystals continue to be laid down on the anterior surface.

4) Juvenile Stage

Returning to what I have seen, it is now in order to speak to the fourth, the Juvenile Stage, in the developmental series. In this stage, the wing is extended upward, connecting with the medial curvature, thereby completing a surface which bears a foramen through the statolith (Fig. 16). Further extension of the wing has resulted in the creation of the medial fissure, which is a discontinuity between the wing ventrally and the dorsal spur dorsally. There is a continuing formation of the occulting crystals. This stage is found in five specimens ranging in size from 109 to 118 mm DML.

5) Adult Stage

The Adult Stage is found in late juveniles and sexually maturing or mature adults (DML over 118 mm) i.e. nearly all I. illecebrosus taken in inshore Newfoundland waters. In the adult statolith, the inferior lateral dome may subdivide so that the entire lateral dome is tripartite

FIGURE 16. Juvenile Stage in the development of the statolith of *Illex illecebrosus* (Lesueur) from a female specimen of 109 mm dorsal mantle length. (Anterior view). Specimen is mounted in glycerine.

Legend: DD Dorsal Dome

DS Dorsal Spur

FM Medial Fissure

F Foramen

LI Inferior Lobe of Lateral Dome

LS Superior Lobe of Lateral Dome

R Rostrum

W Wing

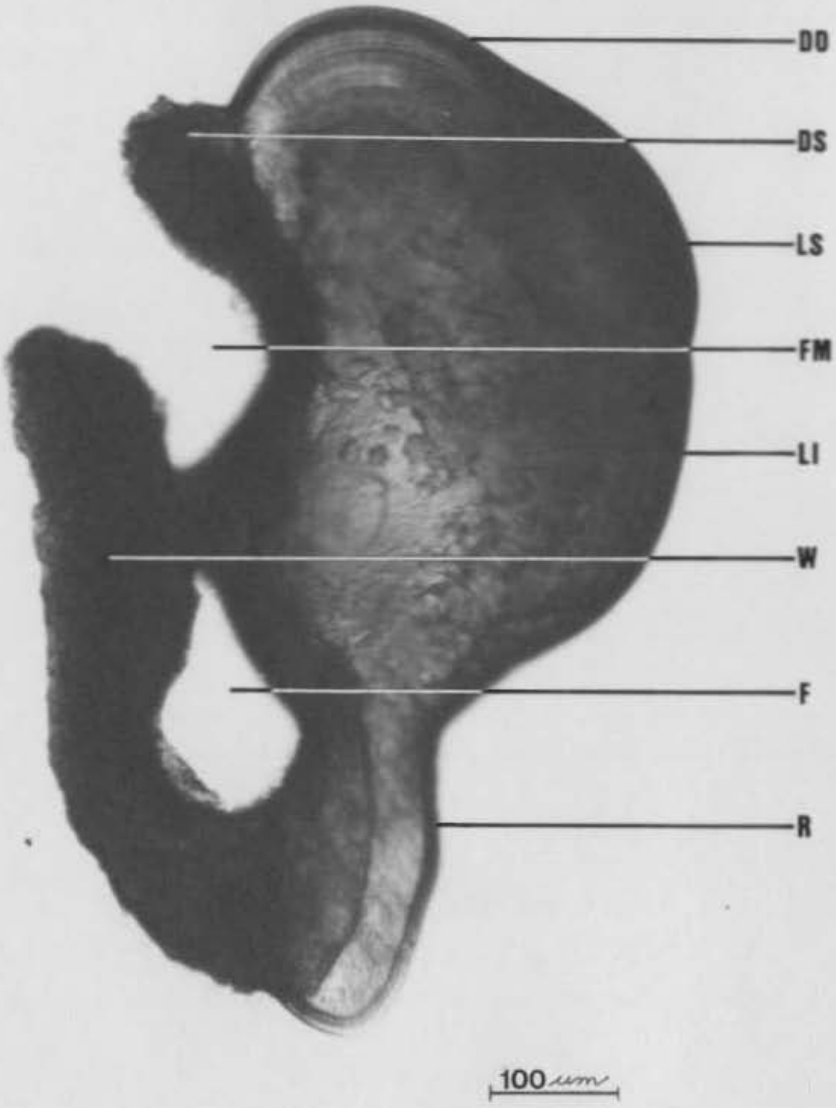
DO
DS
LS
FM
LI
W
F
R
100 um

(Fig. 17). The foramen gradually becomes filled through the deposition of crystals and the medial fissure similarly narrows. Irregular occulting crystals cover most of the anterior surface of the statolith in this stage, with the exception of the immediate area of the nucleus. It should be noted that these crystals are most concentrated in the region of their genesis, indicating their continual production and deposition in that area, despite their area of deposition being enlarged with age and over a period of time.

6) Advanced Stage

In the Advanced Stage of statolith development (Fig. 18), the appearance is similar to that of the adult except that the foramen and the medial fissure are closed, having been filled by crystalline deposition. The lateral dome may or may not be tripartite; indeed, right and left statoliths from the same animal have been seen to vary in having the tripartite condition of the lateral dome in one but not in the other. I have observed varying degrees of transition between the adult and the advanced stages, but none as developed as the particular specimen illustrated.

As the growing statolith passes through the developmental stages, changes in the pattern with which the increments are deposited are visible. These patterns are characteristic of different parts of that portion of the statolith composed of regularly arranged crystals.

The Advanced Stage appears in squid of minimum DML of 230 mm.

C. Regions of Statolith

The nucleus of the statolith consists of the innermost prominent dark lamella and its contained lighter region, the kernel.

FIGURE 17. Adult Stage in the development of the statolith of Illex illecebrosus (Lesueur) from a female specimen of 244 mm dorsal mantle length. (Anterior view). Specimen mounted in glycerine.

Legend: DD - Dorsal Dome

DS - Dorsal Spur

FM - Medial Fissure

F - Foramen

LI - Inferior Lobe of Lateral Dome

LM - Medial Lobe of Lateral Dome

LS - Superior Lobe of Lateral Dome

R - Rostrum

W - Wing

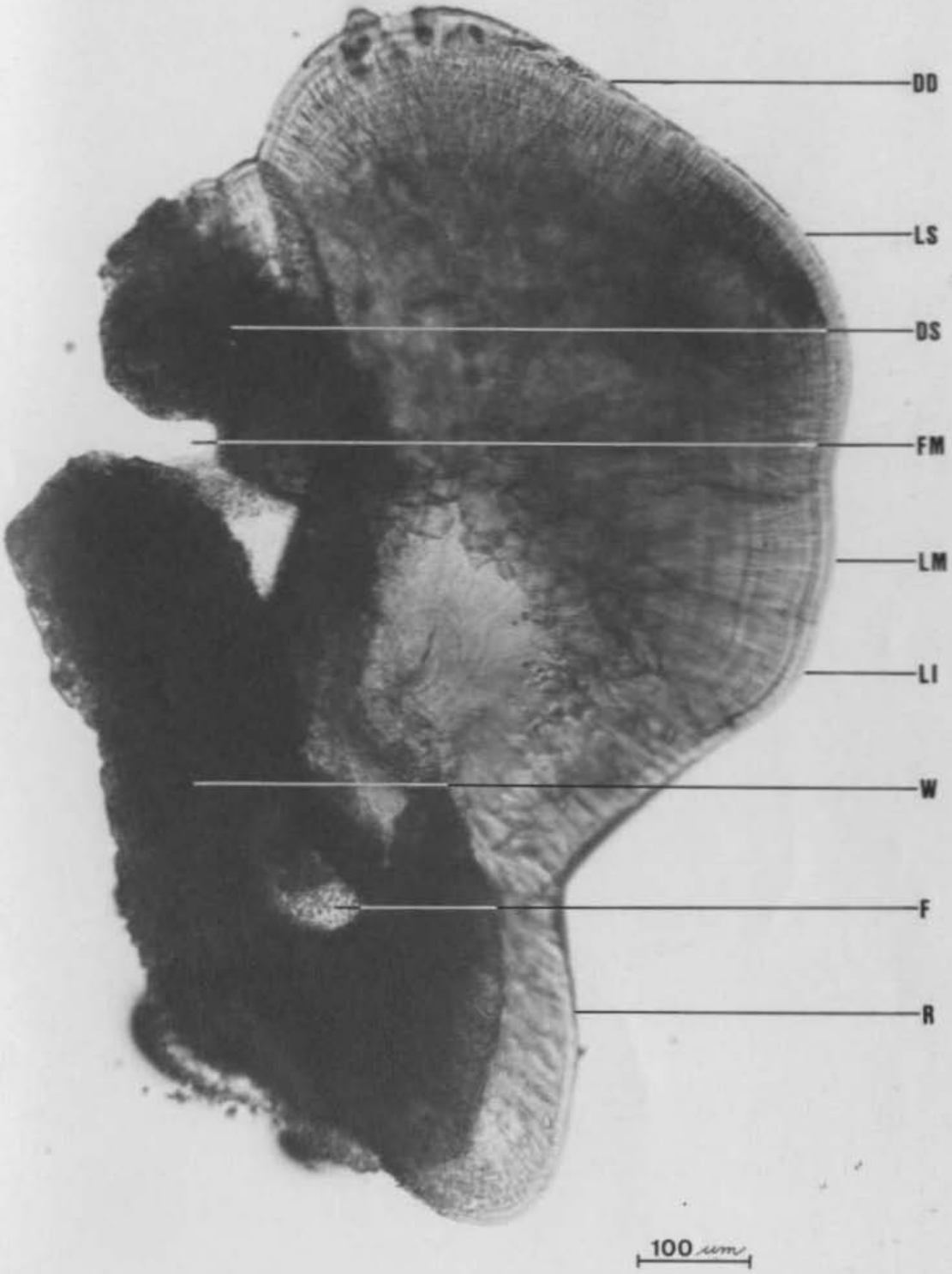
DD
LS
DS
FM
LM
LI
W
F
R
100 um

FIGURE 18. Advanced Stage in the development of the statolith of *Illex illecebrosus* (Lesueur) from a mature male specimen of DML 230 mm (Anterior view) Specimen mounted in glycerine.

Legend: DD - Dorsal Dome

FM - Medial Fissure

LI - Inferior Lobe of Lateral Dome

LS - Superior Lobe of Lateral Dome

R - Rostrum

DS - Dorsal Spur

W - Wing

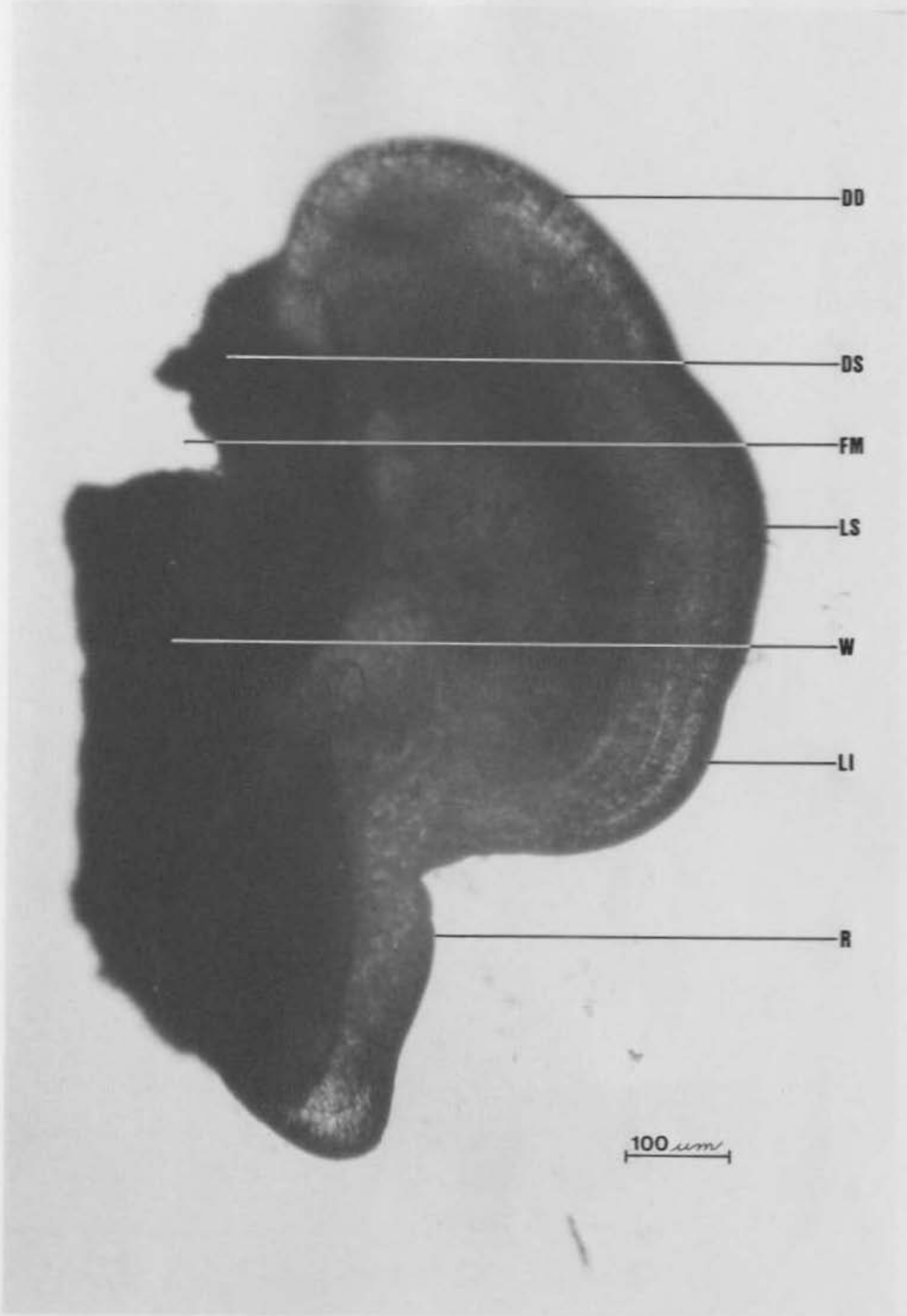
DD
DS
FM
LS
W
LI
R
100 um

Beyond the nucleus, three distinct growth regions, as delineated by observed growth increment patterns, were identified and are herein designated as Region 1 (R1), Region 2 (R2) and Region 3 (R3) (Fig. 19). Quantitative descriptions of these regions are given in Table 3 and their positions on the statolith in Figure 19.

The first region (R1), immediately peripheral to the nucleus, is characterized by narrow and closely spaced rings with more prominent rings occasionally interspersed among them (Fig.20). In the smallest specimens, this is the predominent region with small initial portions of R2 beginning to be laid down on its periphery.

At the inner margin of R2 the direction of maximum growth of the dome anlage shifts some 35° toward the dorsal midline. This region is characterized by increments and rings of irregular widths with the widest increments occurring at the inner margin of R2. The increments throughout R2 are generally wider than those found in R1 and the rings vary in darkness. Noticeably darker rings often occur with a pattern of one dark ring followed by a series of seven, or a multiple of seven lighter rings. In Figure 21 is illustrated an example where this sabbatical periodicity can be traced through most of the statolith.

The third region, R3, is found only in statoliths from the older specimens examined, and is found around the outer periphery, excluding the wing areas of random crystalline arrangement. Increments in R3 are narrow and the rings are thin and evenly spaced. The occurrence of prominent dark increments is reduced and in some cases is even absent. Where they do occur, patterns of seven and fourteen are again sometimes seen.

FIGURE 19. Ground anterior surface of an EPON 812 embedded statolith of Illex illecebrosus (Lesueur) to show the three regions of increment formation and the position of the occulting crystals. Taken from a male specimen of 168 mm dorsal mantle length.

Legend: CO - Occulting Crystals

R1 - Region One

R2 - Region Two

R3 - Region Three

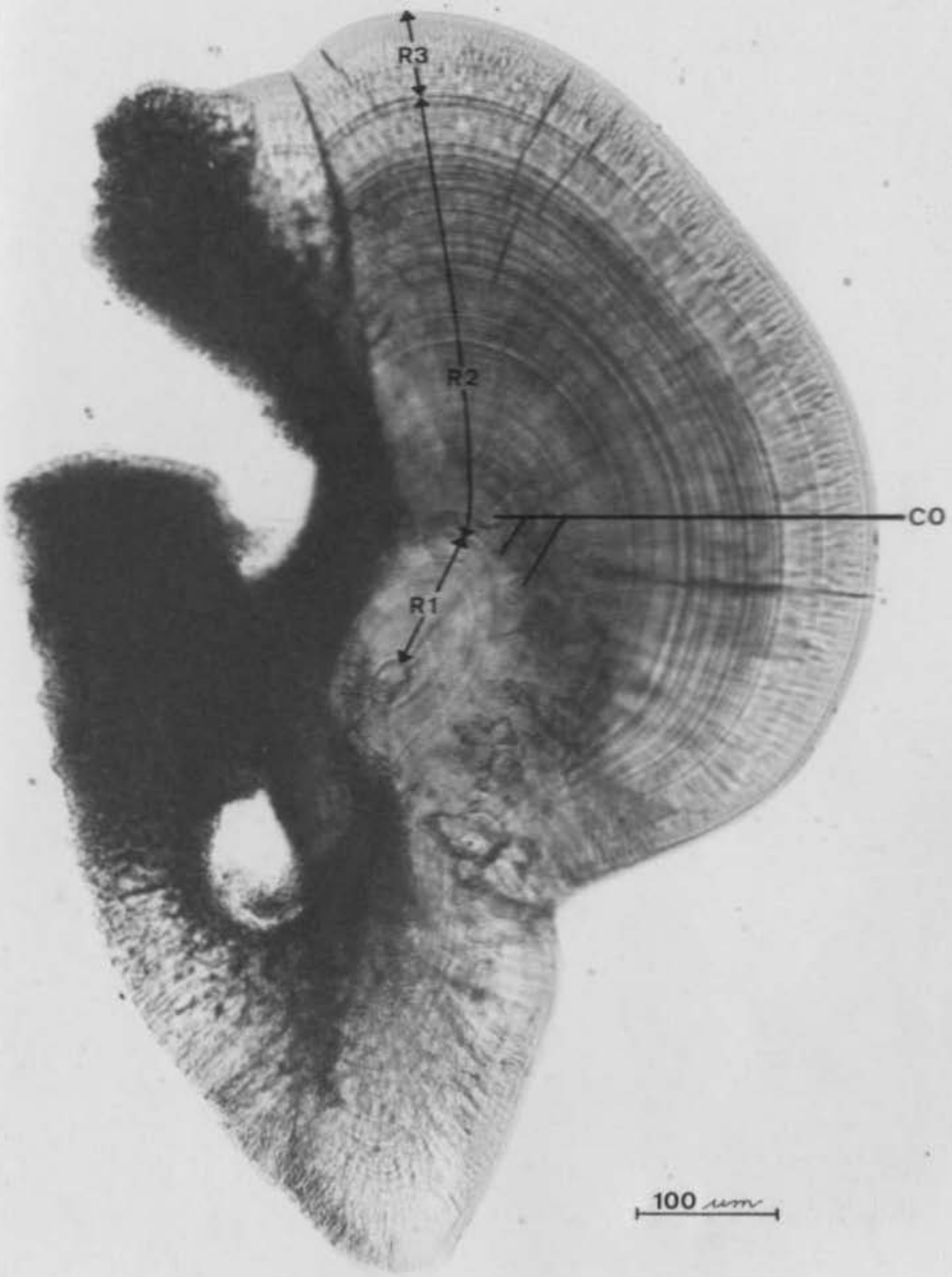
R3
R2
CO
R1
100 um

TABLE 3. Mean measurements and ranges of increment widths and regional widths from seven statoliths from seven female specimens of *Illex illecebrosus* captured in October, 1981. All statoliths used in these data exhibited growth typical of region three (R3). Specimens are listed in Table 4.

Region	Mean Increment Width (μm)	Range of Increment Width (μm)	Mean Region Width (μm)	Standard Deviation of Region Width (μm)	Range of Region Width (μm)	Mean Number of Increments	Standard Deviation of Number of Increments	Range of Number of Increments
Nucleus	-	-	17.8	1.5	15-21	-	-	-
R 1	3.0	2.5-3.5	122.0	9.5	109-139	40.1	7.8	30-51
R 2	3.4	1.5-5.0	403.0	22.5	378-431	127.1	7.9	97-140
R 3	2.3	2.0-2.6	112.0	10.5	98-122	50.6	8.7	40-65

FIGURE 20. Diagrammatic representation of tracing of growth increments in statolith (length 1023 μm) of Illex illecebrosus (Lesueur) (DML 226 mm), indicating the three regions of growth, designated R1, R2 and R3.

N - Nucleus

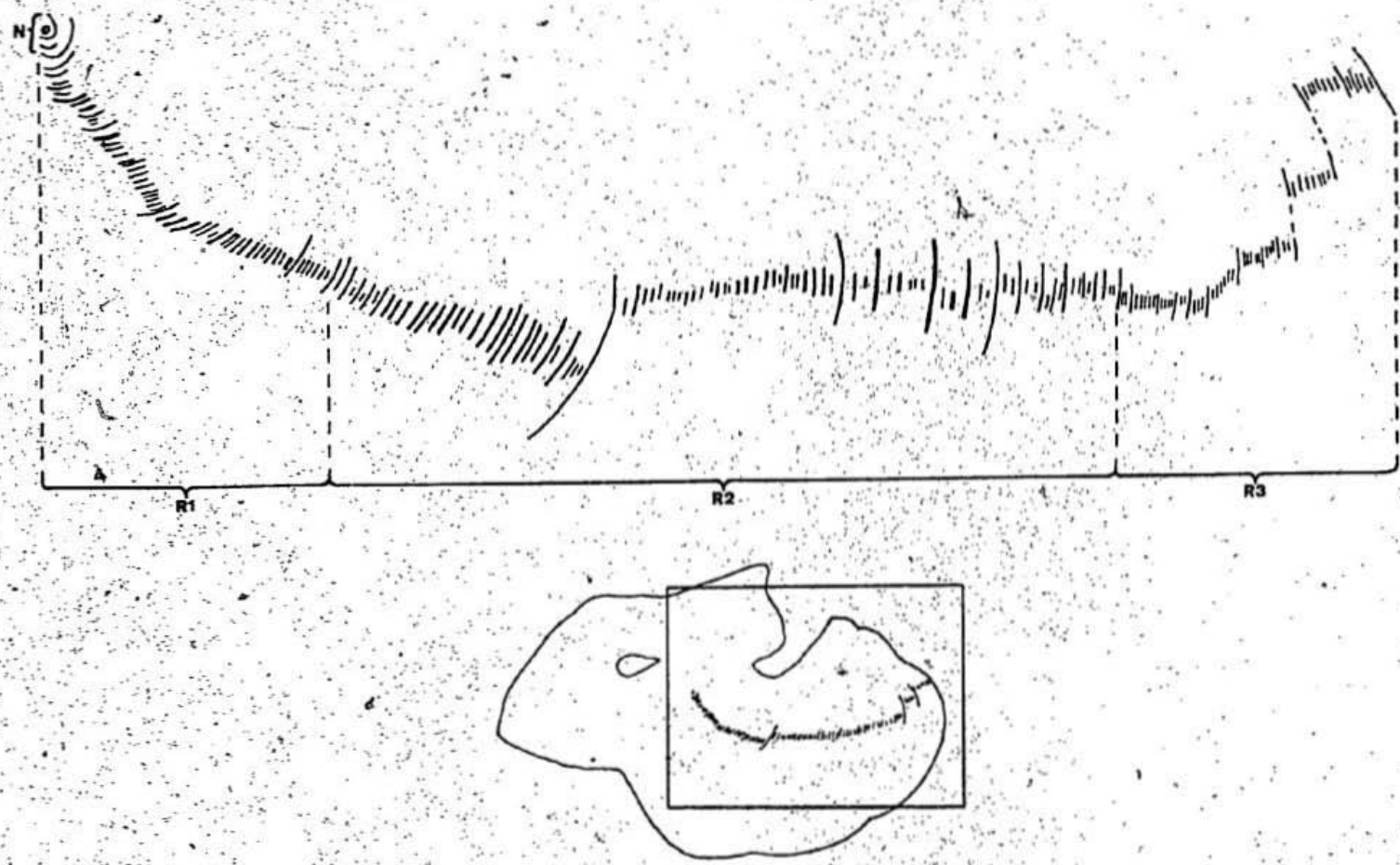
N
R1
R2
R3

FIGURE 21. Diagrammatic representation of tracing of growth rings in a statolith (length: 997 μm) of a male *Illex illecebrosus* (Lesueur) (DML: 212 mm).

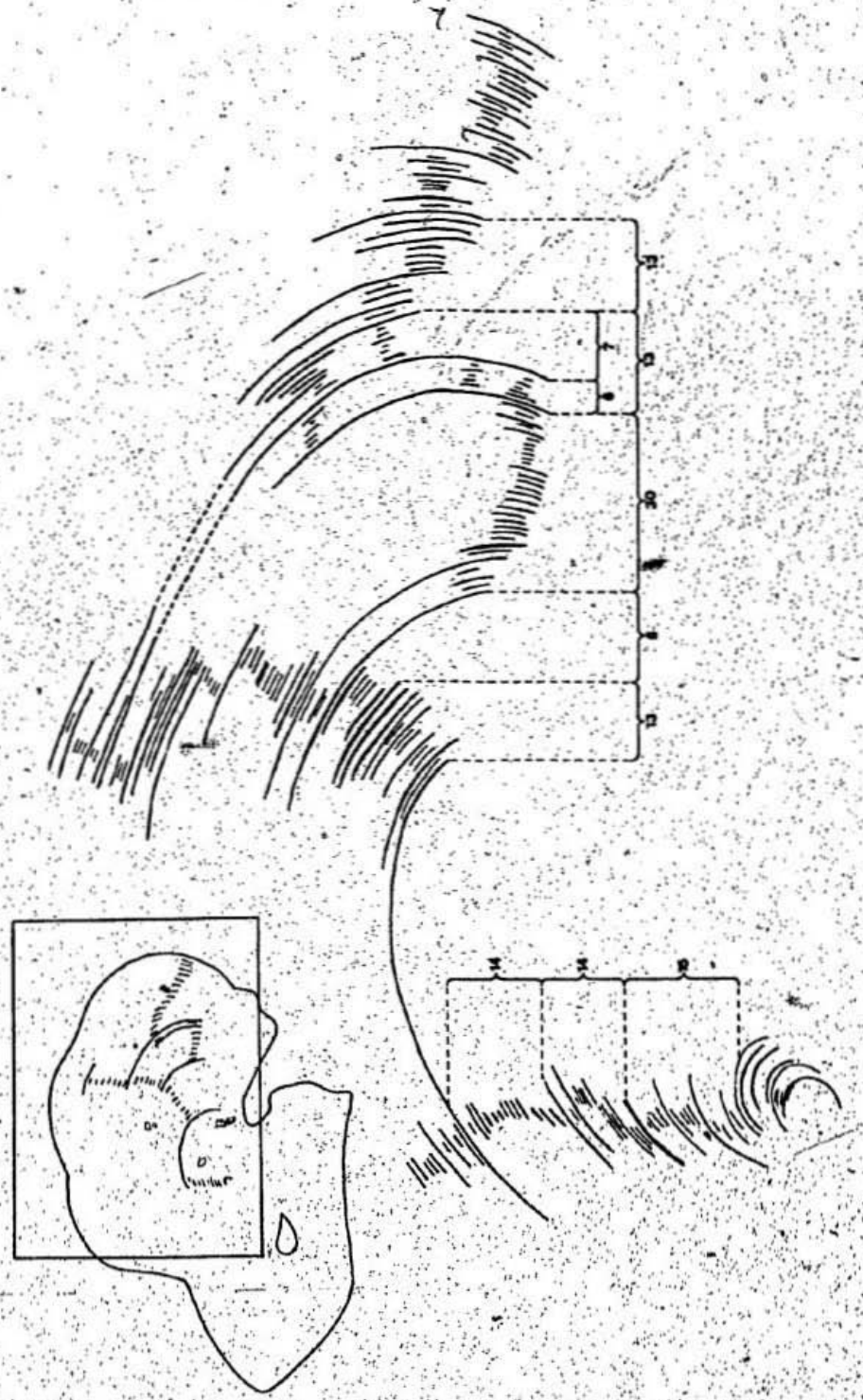

D. Increments, Their Counts and Their Analysis

During the counting of the increments it was usually found that at least two of the three mandatory minimum three increments counts had variations of no more than the acceptable 5% limit. Greatest variations (up to 22%) occurred during observer fatigue or during the first one or two counts during a day.

Plots of numbers of increments against statolith length, dorsal mantle length (DML) and date of capture of the squid are presented as Figures 22, 23 and 24. Plots of statolith length against DML and date of capture are presented in Figures 25 and 26. The collected data for these graphs are given in Tables 4, 5 and 6. Reference to Figures 27 and 28 will indicate the appearance of the growth increments in the region of the dorsal dome. With particular reference to Figure 28, the dark and light portions of a single increment are clearly evident in stereo micrographs at a magnification of 2200X.

Analysis of variance, two sample t-test, and Mann-Whitney test showed no significant difference between the first three counts of stained specimens and three counts of unstained specimens at the .05 level of significance. These analyses were performed on eight female specimens (Table 4). However, this does not rule out the qualitative increase in the visibility of the increments, i.e. although there is no significant increase in the number of increments counted, those which are counted are more easily seen by staining.

E. Technical Comments

In the early phases of this work and in the preparation of specimens, it was found that those glues which hardened by the

evaporation of the solvent were not suitable for use as mounting media. They did not allow clear viewing of the growth increments within the statoliths. "Diatex" mounting cement, Canada balsam, Turtox mounting medium, liquid acrylics, clear nail polish and various "super glues" were tried and rejected for this reason.

Polymerizing epoxy cement permitted viewing of increments, but was unmanageable to work with because of its quick-setting quality and because it is difficult to mix with consistent proportions in the small quantities required in work of this sort. The mountant known as EPON 812 (Fisher Scientific Limited), which is polymerized by heat, was found to be of sufficient optical quality and ease of handling for use in the preparation of statoliths for observation and analysis.

Although grinding the statoliths was required to facilitate viewing of increments in juvenile and adult specimens, grinding increased obscurity of increments in larval specimens.

Statoliths from male specimens are more difficult to successfully mount and grind to allow clear viewing of growth increments throughout the counting range than are statoliths from female specimens.

FIGURE 22. Relationship between statolith length and number of increments in the statolith of *Illex illecebrosus* (Lesueur). Data from Tables 4 and 6.

$Y = 0.1878\ X + 4.6$

$n = 31$

$S^2y.x = 153.4$

$r = 0.980$

$t = 2.042$

$x^2 = 3164172$

$\bar{X} = 661$

— — = Regression of the model to x = 0

— — — = limits of 95% confidence interval of the model

(Calculations and symbolism as from Zar, 1974)

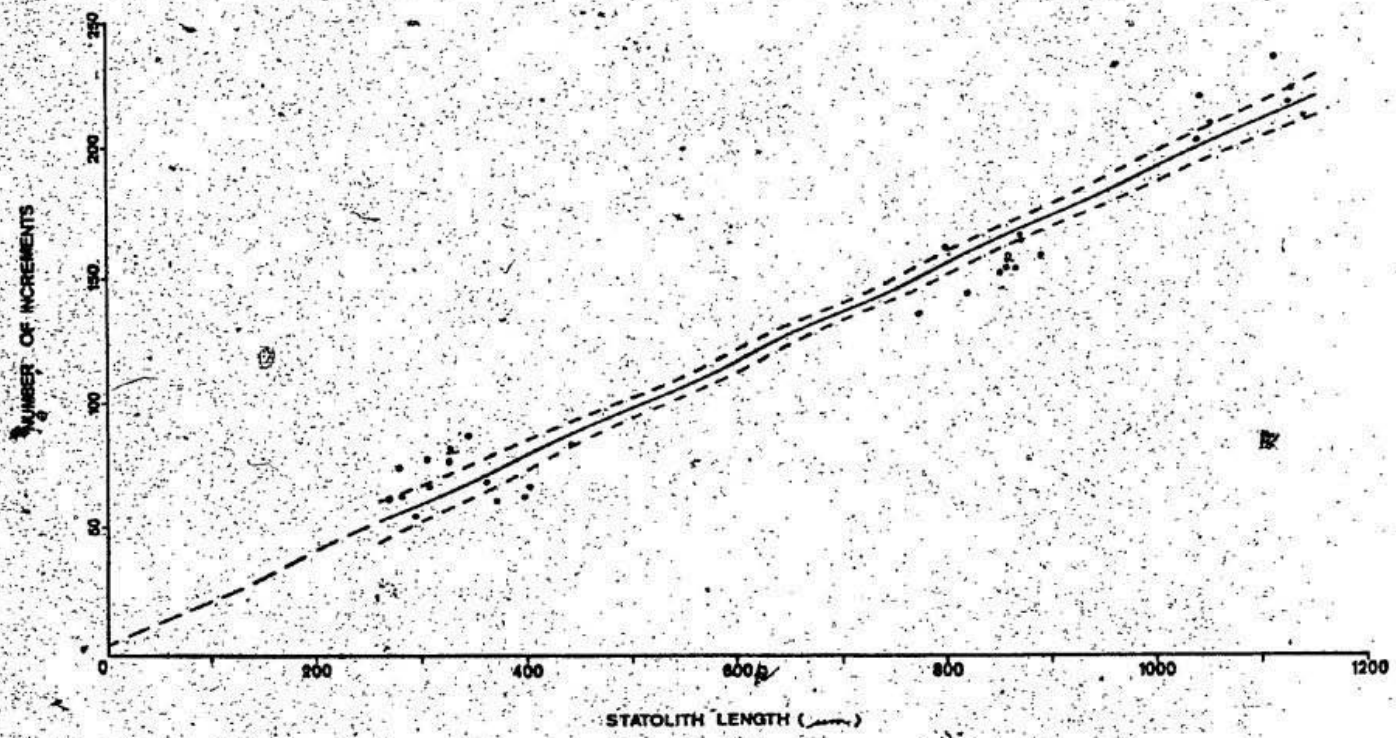
NUMBER OF INCREMENTS
0
50
100
150
200
250
200
400
600
800
1000
1200
STATOLITH LENGTH (μm)

FIGURE 23. Relationship between dorsal mantle length and number of increments in the statolith of *Illex illecebrosus* (Lesueur). (Data from Tables 4 and 6)

$Y = 0.625X + 60.1$

$n = 31$

$S^2_{Y.X} = 119.2$

$r = 0.984$

$x^2 = 274879$

$\bar{X} = 115.3$

$t = 2.093$

— — — = Limits of 95% confidence interval for the model.

(Calculations and symbolism as from Zar, 1974)

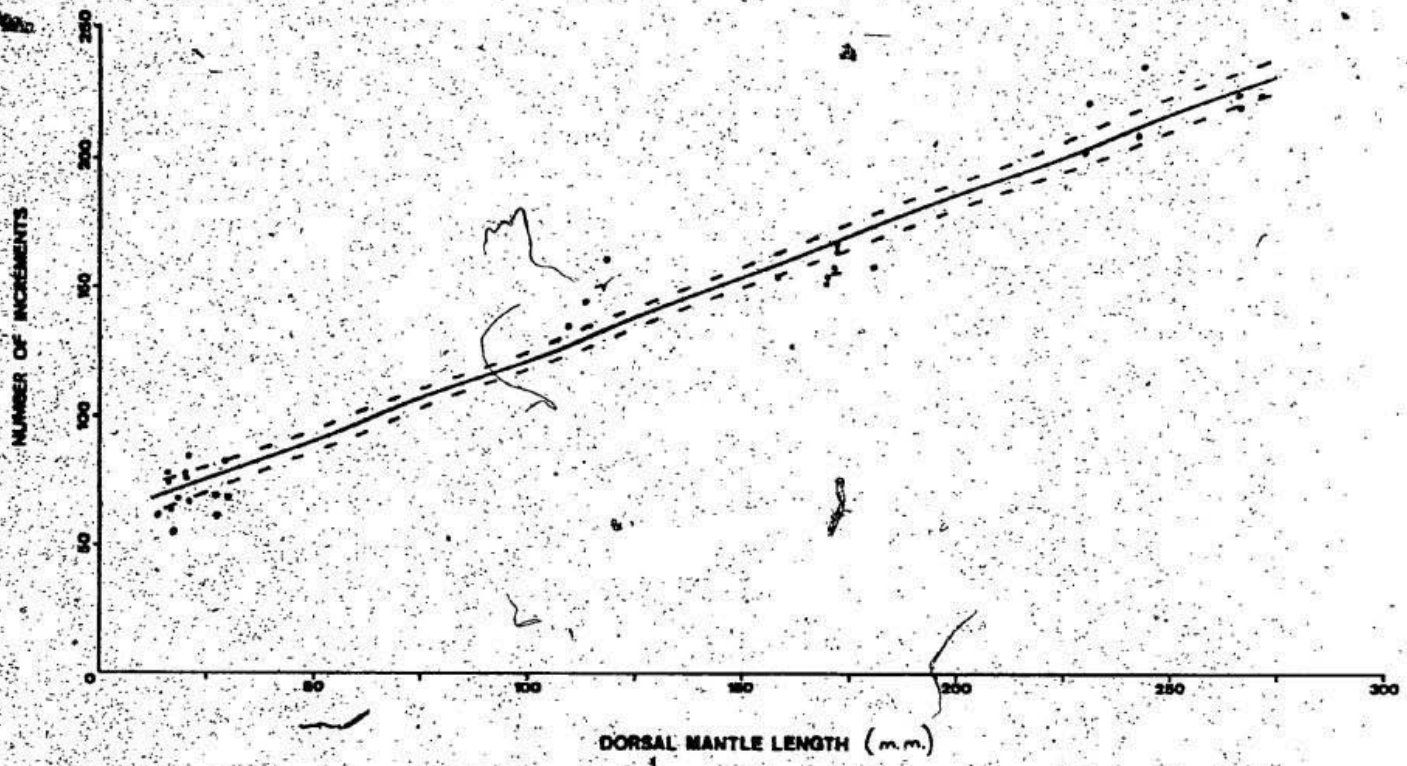
NUMBER OF INCREMENTS
0
50
100
150
200
250
50
100
150
200
250
300
DORSAL MANTLE LENGTH (m.m.)

FIGURE 24. Graph of Von Bertalanffy growth relationship between date of capture and number of increments in the statoliths of Illex illecebrosus (Lesueur). (Data from Tables 4 and 6)

Model: $Lt = L_\infty(1 - e^{-k(t-t_o)})$

Where Lt = Number of increments at time (t)

L_∞ = Number of increments at t = infinity

e = Base of natural logarithms

K = Growth constant

t_o = Time at which increments begin to form

And where $L_\infty = 357.5$

$e = 2.7183$

$K = 0.09711$

$t_o = -0.3860$

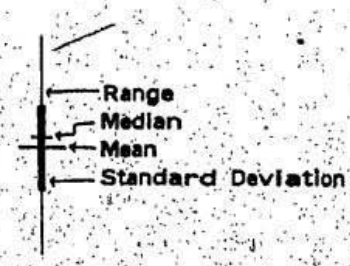

(Calculations and symbolism as from Ricker, 1975)

NUMBER OF INCREMENTS
50
100
150
200
250
MONTH
F
M
A
M
J
J
A
S
O
N
D

FIGURE 25. Relationship between dorsal mantle length and statolith length in *Illex illecebrosus* (Lesueur) (Data from Tables 4 and 6, regression calculated for data from adult female specimens only, Table 4)

$Y = 2.33X + 196$

$n = 17$

$S^2_{y.x} = 916.8$

$r = 0.974$

$x^2 = 47349$

$\bar{X} = 192.9$

$t = 2.131$

— — = Regression of model to X = O

— — — = Limits of 95% confidence interval for for the model.

(Calculations and symbolism as from Zar, 1974).

(Note that the data from larval specimens lie outside the 95% confidence interval of the model.)

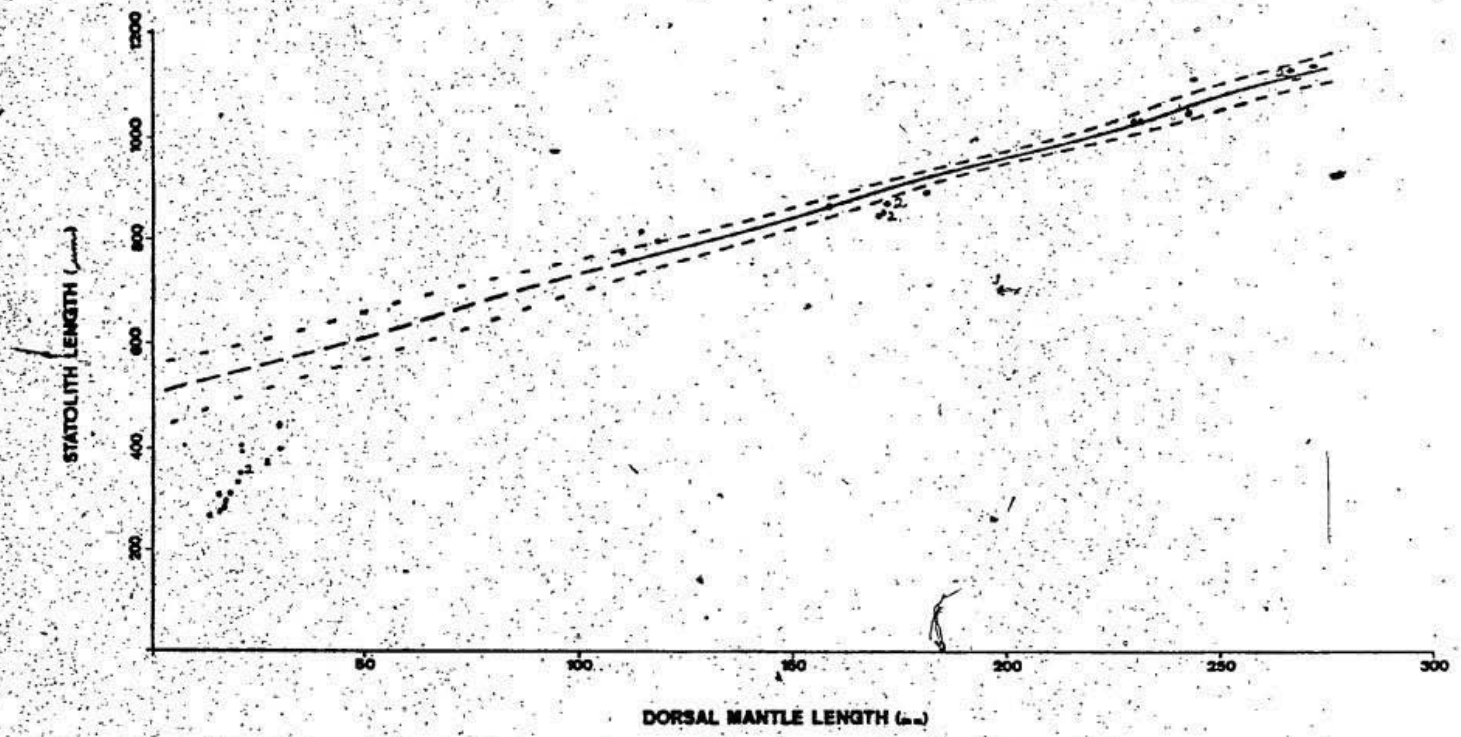
STATOLITH LENGTH (mm)
200
400
600
800
1000
1200
50
100
150
200
250
300
DORSAL MANTLE LENGTH (mm)

FIGURE 26. Graph of Von Bertalanffy growth relationship between date of capture and statolith length of *Illex illecebrosus* (Lesueur). (Data from Tables 4 and 6)

$$Lt = L_{\infty}(1 - e^{-k(t - t_o)})$$

Where Lt = Length of statolith at time (t)

L_{∞} = Length of statolith t = infinity

e = Base of natural logarithms

K = Growth constant

t_o = Time at which increments begin to form

L_{∞} = 1228

K = 0.2482

t_o = 0.6802

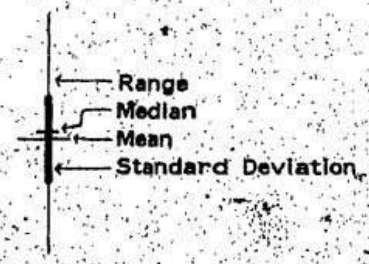

(Calculations and symbolism as from Ricker, 1975).

STATOLITH LENGTH (μm)
200
400
600
800
1000
1200
MONTH
M
A
M
J
J
A
S
O
N
D

TABLE 4. Data (as counts of increments in ground statoliths) of seventeen statoliths from fifteen specimens of female *Illex illecebrosus* (Lesueur)

Specimen	Statolith Length	Dorsal Mantle Length	Unstained Ground Statolith Increment Counts			Ninhydrin/Fast Green Stained Ground Statolith Increment Counts					Final Accepted Count Value	Date of Capture (1981)
141R	1139	271				213	202	215			214.0	Oct. 13
142R	1049	242				206	209	210			209.5	Oct. 13
143L	1126	266				215	222	227			224.5	Oct. 13
145R	1038	229				190	207	200			203.5	Oct. 13
147L	1039	231				175	168	224	219		221.5	Oct. 13
197R	889	181				159	158	154			158.5	June 20
201R	864	158				153	143	155	154		154.0	June 20
205L	870	172	140	155	148	151	170	162			166.0	June 20
205R	870	172	128	153	147	152	160	168			164.0	June 20
210L	856	170	128	131	137	142	143	149	153	154	153.5	June 20
210R	856	170	120	135	134	153	140	144	152	155	154.0	June 20
212R	851	169				150	151	153			152.0	June 20
219R	1110	243				191	195	237	236		236.5	Oct. 13
229R	1124	266	170	210	219	219	219	219			219.0	Oct. 13
232L	798	118	143	146	132	145	152	162	160		161.0	May 25
234L	772	109	127	159	152	135	142	135	135	136	135.0	May 25
237R	818	113	142	135	139	135	145	143			144.0	May 25

L – Left statolith
R – Right statolith

Specimen	Statolith Length	Dorsal Mantle Length	Ninhydrin/Fast Green Stained Ground Statolith Increment Counts				Final Accepted Count Value	Date of Capture (1981)
120L	1139	236	192	199	202		200.5	Oct. 13
123L	1045	218	192	201	214	211	212.5	Oct. 13
123R	1045	218	197	201	199		200.0	Oct. 13
154R	1023	226	200	216	214		215.0	Oct. 13
169R	937	165	148	164	160	155	162.0	June 20
169L	937	165	152	155	165	167	166.0	June 20
171R	933	180	155	139	150	158	156.5	June 20
171L	933	180	158	162	170	174	172	June 20
194L*	-	169	171	176	176	167	176	June 20

*Rostrum broken

TABLE 5. Data (as counts of increments in ground statoliths) from nine specimens of male Illex illecebrosus (Lesueur).

TABLE 6. Data (as counts of increments in whole statoliths) of sixteen statoliths from twelve larval specimens of *Illex illecebrosus* (Lesueur)

Specimen	Statolith Length	Dorsal Mantle Length	Increment Counts of Unstained Entire Statoliths					Final Accepted Increment Count	Date of Capture (1981)
1 L*	390	21	-	-	-	-	-	-	Mar. 4
1 R	403	21	70	65	67	-	-	66.0	Mar. 4
2 L	397	30	57	69	67	-	-	-	Mar. 4
2 R**	-	30	-	-	-	-	-	-	Mar. 4
3 L	371	27	60	62	61	-	-	-	Mar. 4
3 R	361	27	66	71	68	-	-	-	Mar. 4
215 L	293	17	54	56	55	-	-	55.0	Feb. 27
117 L	281	16.5	58	61	64	-	-	63.0	Feb. 27
238 R	442	29	89	71	95	83	84	83.5	Feb. 27
239 L	268	13.5	65	61	77	60	63	61.5	Feb. 27
240 R	278	16	56	54	75	74	-	74.5	Feb. 27
241 L	326	20	55	66	79	75	-	77.0	Feb. 27
242 R	344	21	73	71	85	85	-	85.5	Feb. 27
242 L	342	21	64	71	77	75	-	76.0	Feb. 27
243 R	305	16	67	52	78	77	-	77.5	Feb. 27
244 L	307	18	52	59	68	67	-	67.5	Feb. 27

* Cracked upon grinding, not included in Figs. 22, 23 and 24

** Lost during dissection

L - Left statolith
R - Right statolith

FIGURE 27. Scanning electron microscope of the Dorsal Dome region of a ground and etched statolith of *Illex illecebrosus* (Lesueur) showing numerous growth increments (500X).

FIGURE 28. Scanning electron micrograph of the Dorsal Dome region of a ground and etched statolith of *Illex illecebrosus* (Lesueur) showing the organic and crystalline portion of the increments (2200X).

O = Organic-rich portion of increment

C = Crystalline portion of increment

I = One increment

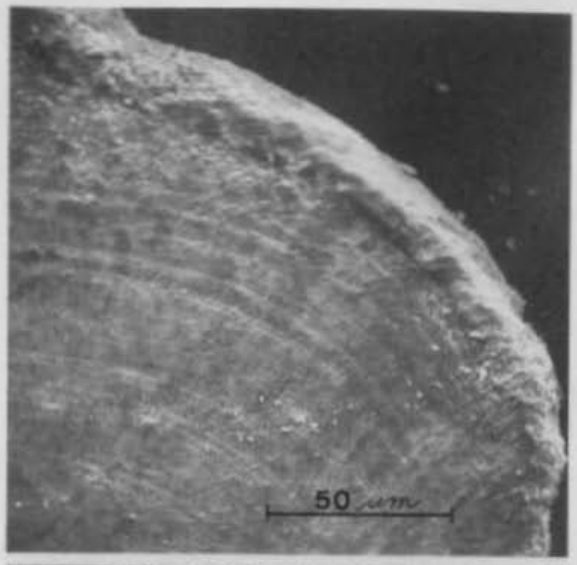
50 um

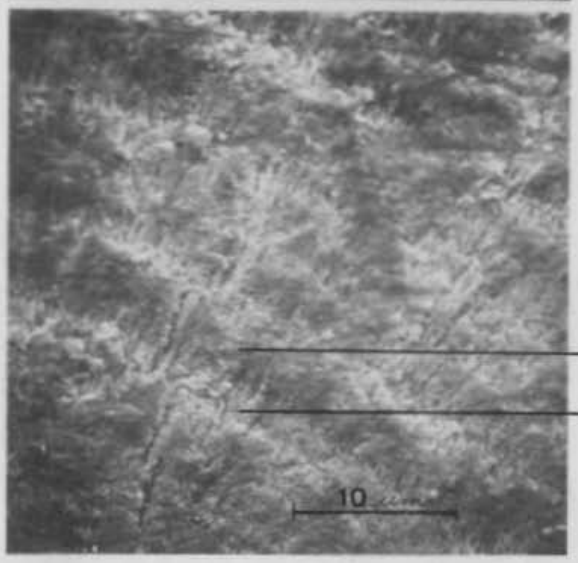
O
C
I
10 um

DISCUSSION

As noted in this thesis and by Lipinski (1980), statoliths from male specimens of the ommastrephid teuthoid Illex illecebrosus have been difficult to prepare for examination of growth increments while those from female specimens can be prepared with a much higher success rate. It may be concluded that there must be some sexually variant cause for this observed difference, yet grossly there has been no success in distinguishing statoliths from male or female squid on the basis of observation alone.

The main problem encountered in specimen preparation was in removing the occulting crystals without severe grinding of the statolith which completely obliterates the growth increments. Ground glass rods, needles, dental picks and drills failed to dislodge these crystals and maintain the integrity of the growth increments. This was true even in specimens where the increments were visible over the entire counting area (except in the area of the occulting crystals). If statoliths are ground sufficiently to remove these crystals, then increments are obscured as a result of the grinding, particularly at the dorsal dome. Physical depression of the dorsal dome during mounting helps prevent the obliteration of increments in that region and, at the same time, enhances the removal of the occulting crystals by grinding. However, certain specimens, though optimally ground, still retain these crystals in sufficient quantities to prohibit successful counting. This can be seen by reference to Figures 11 & 12. In specimens in which growth increments are obscured by superficial crystalline deposits, the occulting crystals penetrate into the statolith to a point, such that

further grinding (i.e., past the point at which the increments are perpendicular to the light path of the microscope) would further destroy evidence of increments.

Using the method described, 67% of specimens from females were found to be countable, while only 45% of specimens from males were found acceptable. Unfortunately, at the time when the method was developed, numbers of male specimens from some of the capture dates and sites were either too few or unavailable. Regretably, due to the small samples available, some statoliths from male squid were expended in the process of developing the method itself and were wasted, as it were, in attempts to perfect appropriate techniques. Subsequent lack of specimens did not provide sufficient data on males. Consequently, all graphic data presented herein pertains to female specimens with the exception of the larvae which, on the basis of current knowledge, could not be sexed.

The method used in counting the increments on the ground statoliths is an original one. It is the first to employ a permanent tracing of a projected image, with the subsequent use of the tracing in the actual counting. Consequently, the increments are not counted directly as in other methods reported, and counting toward an expected number of increments, however unconsciously, for a particular size of structure bearing the increments is avoided and obviated. The tracing remains as a record of the increments, and of the counting, and thus enhance reproducibility.

Because growth increments in different areas of the statolith lie in different focal planes, the counting of these increments requires continuous focusing of the microscope. The obvious limitation of the

use of a photographic record is that it is restricted to a single focal plane. The tracing, as here employed, permits the recording of information gleaned from an analysis of a statolith. Therefore, it is contended that the methods developed and reported herein have decided advantages over those which rely either upon entirely visual counts, or upon the capture of photographic images.

The counting method presented in this thesis has other definite advantages over those reported from studies involving other mollusca, fish and annelids (e.g., Kennish (1980) Pannella (1980), and Olive (1980)). These are, (1) the small space required for such work, (2) limited expense, since the only required equipment is a microprojector, surface-coated mirror and a dark adapted area, (3) no time or chemicals are required for photographic processing, (4) counting bias is eliminated, (5) a permanent record exists, (6) preparation of SEM material to view increments is not necessary unless specifically desired, (7) the results are reproducible and the use of tracings make counting errors less likely then with the use of a microscope alone, (8) teaching the technique requires minimal instruction and (9) the tracings hold a representation of the history of the animal. The obvious flaws in the technique are that the counts are subject to fatigue and lack of practice on the part of the person who makes the tracings.

It is also of significance to note that Methven (1983) has been able to utilize this tracing method to age the hake Urophycis chuss (Walbaum) and the method also holds promise for ageing U. tenuis (Mitchill).

An admitted exception to the benefits of using this method occurs when unusually clear increments are visible on a single plane and /or

are best viewed by electron microscopy, as in the case of Evans (1972) who examined shells of the cockle Clinocardium nuttalli.

During certain years, the size distribution of each sex of Illex illecebrosus in the inshore waters of Newfoundland is bimodal (Squires, 1957). This bimodality appears to occur every two years (Squires, personal communication). During late summer, 1980, this author noted squid from Conception Bay of smaller mantle lengths than those present in the bay one month previously, thus indicating that 1980 was a year characterized by a bimodal size distribution. It is thus fortunate that the specimens used in this study were collected in 1981 and therefore probably represent a single size class. However, 1981 was a year of poor abundance of squid in inshore waters and samples were not available for long periods during the inshore fishing season. Consequently, the samples are not uniform, or even random, but are opportunistic.

The number of increments seen in ground statoliths of Illex illecebrosus increases with statolith length (Fig. 22), dorsal mantle length (Fig. 23) and over time (Fig. 24). These relationships are reasonable evidence that the increments referred to in this discourse are true growth increments, i.e., they are a record of periodic, rather than aperiodic changes in the physiology of the animals.

Clearly, the statolith enlarges by the addition of growth increments and its shape appears to be initially determined by the macula (Stephens and Young, 1982). Statolith shape is species-characteristic (Clarke, 1978) and is probably indicative of the locomotive and manoeuvering ability of the species of squid (Stephens and Young, 1982). However, the specific factors which influence the

shape of the statolith are unknown, as is the mechanism of increment formation. In bivalve and gastropod molluscs, the growth increments of the shell are created by secretions of the cells at the mantle margin. In cephalopods, however, the increment-forming surface of the statolith has no closely applied cellular layer and presumably increment formation occurs as a function of the concentration of dissolved calcium carbonate in the statolymph, with increasing concentration causing calcium deposition on the statolith. A similar acquisition of crystals has been described for spicules of the sponge Leucosolenia complicata (Minchin) left in a calcium carbonate solution (Jones, 1955) where crystals are deposited along the same axes as those of the crystal of the spicule itself. This may help explain why the regularly arranged crystals of the statolith continue their arrangement in subsequent increments but it still does not explain the origin of the crystal arrangement or the means by which the final shape of the statolith is determined. Radtke (1981) suggests that the organic component of the statolith acts as a template for crystal formation, but this does not explain how or why the final definitive shape is attained.

The groupings of 7, 14 or 28 increments are typically associated with lunar (i.e., tidal) periodicities. In many fish species, such as the silver hake Merluccinus bilinearis (Mitchill), such patterns occur as six or seven narrow increments alternating with six to eight wider ones, both of these groupings occurring in a repeating 14-increment-series (Pannella, 1980). Both Kristensen (1980) and Rosenberg, et al (1981) have found similar patterns consisting of 14 light (i.e., with a narrow ring) increments followed by 14 darker increments, together forming a repeating series of 28 increments, in Gonatus fabricii (Lichtenstein) and Todarodes sagittatus (Lamarck) respectively. These groupings do not

correspond to those found in I. illecebrosus. However, patterns consisting of groups of 7, 14 or 28 increments separated by single prominently lighter or darker increments have been seen in the reef dwelling hogfish Lachnolaimus maximum (Walbaum) and in the doctorfish Acanthurus chirurgus (Bloch) (Pannella 1980). In the estuarine English sole Parophrys vetulus Girard, one prominent dark increment is formed after thirteen lighter ones (Rosenberg, 1982). These patterns parallel those reported here in I. illecebrosus.

It is unfortunate, however, that the variability in increment widths is so great and irregular, especially in R2 of I. illecebrosus, as to obscure the sabbatical periodicity. Dark increments may be often found amidst series of seven increments, as well as at the ends of series. This suggests strong environmental influences on increment formation which may possibly originate from changes in temperature, salinity, or depth and/or as a result of predation, pursuit, illness or other biologically imposed causation. The sabbatical periodicity, although obscure to some, can be found if sought, and is well within acceptable ranges for increment periodicities in other light forms.

The graph of number of increments plotted against date of capture (Fig. 24), is calculated as a curvilinear relationship. However, the curve itself is very gentle and approximates a straight line. The average slope of this curve between late February and June 20th yields an estimate of the rate of growth increment formation of nearly one increment per solar day (26 increments per 31 solar days). The rate indicated for the smallest specimens collected in late February and early March was 27 increments per 31 solar days. The increment formation rate represented by the largest specimens collected in mid-October was 14 increments in 31 solar days. If one assumes a perfect correlation

between the 24 hour 50 minute theoretical tidal cycle (due to lunar periodicity) and increment formation, the expected number of increments per 31 day-period is 28.9. This compares favourably with the calculated rates for February to March(27 increments per 28.9 lunar days) and February to June (26 increments per 28.9 lunar days), and indicates a daily rate of formation probably based upon tidal periodicity. The increment formation rate in statoliths of squid captured in October becomes one increment per two days, i.e., a bidaily rate.

The assignment of a bidaily rate of increment formation is based upon the assumption that the rates of increment formation follow a growth curve, i.e., the rate changes as the animal ages. Although larval growth rates and rates of increment formation may differ significantly from those of later developmental stages in fishes (Pannella, 1980), the postlarval growth increments typically follow regular predictable patterns. In I. illecebrosus, however, the arrangement of growth increments in R3 (the region being formed in specimens collected in October) the growth increments are closely spaced, most probably due to decreased feeding. This may result in either (1) a true bidaily rate of formation, (2) the non-recording of certain days such that an average of half the number of days is recorded, or (3) decreased increment counts due to difficulties in resolving some of the finer increments in R3. A more detailed discussion of R3 is presented elsewhere in this work (pp. 92, 102-103).

Further with regard to Figure 22, the number of increments in the statoliths bears a direct relationship to the size of the statolith. Extrapolation of the regression line to the y-axis gives an intercept

near zero, i.e., there are no increments when there is no statolith and vice versa. Although the later statement is not completely true due to the presence of the small kernel of the statolith before increments are formed (which is to be discussed later), the zero intercept helps reinforce the general reliability of the graphic model. Although Lipinski (1980) also plotted numbers of increments in the statoliths against DML, he only had nine statoliths with clearly visible increments over the entire counting area and these statoliths were taken from a limited size range of DML from 67 to 146 mm. He also failed to plot his data points and simply presented the relationship itself. The data I present more than double his range, extending into the larval stages, and utilize more than three times the number of specimens.

In the range of data points between 750 and 900 µm statolith length, the greater proportion of data points lie below the regression line. All the specimens in this statolith size range were in the late R2 phase of statolith growth. The R2 growth phase is typified by wide growth increments and this width yields a statolith which is larger than its expected size as predicted by the regression line and consequently, the points lie below the line.

The opposite effect can be noted for the largest statoliths, i.e., of lengths exceeding 1000 µm. Those statoliths were in the R3 growth phase, the phase characterized by very narrow increments. If R3 is sufficiently developed, more increments are deposited per unit of length of statolith growth than as would be predicted if the growth were truly linear. As a result, the data points for statolith specimens exceeding 1000 µm in length lie slightly above the prediction line. It may be further stated that because of the different incremental widths being characteristic of different regions, a more accurate assessment of

the shape of this graph is a slight sigmoid curve, rather than a straight line, even though the linear model apparently fits the data quite well (r= 0.984).

The plot of statolith length against dorsal mantle length (Fig. 25), shows a linear relationship for specimens between 100 mm and 275 mm DML. Although Lipinski (1980) plotted statolith length against DML and found a logarithmic relationship, he only had sufficient data above 120 mm DML where a straight line could fit his data points equally well. Unfortunately, he did not have enough specimens of smaller sizes to observe phenomena which I have seen and now discuss.

The larval specimens lie well below the extrapolated line and indicate that the relationship of statolith length to DML is curvilinear in the early stages of development. In fact, a growth curve could not be fitted to the data for this graph due to change in the growth coefficient (K). K may be constant in the portion of the graph near the origin if that portion is curvilinear. However, the linear portion of the graph, by being linear, indicates a K value which is continuously changing. Even if we assume the early relationship between statolith length and DML to be linear also, we still get different rates of change in K (i.e., different growth rates) between the very small specimens and the juvenile and adult specimens.

Changes in growth coefficients and rates are used to distinguish larval phases of fishes (Nesis, 1979) and the change noted herein may also herald the onset of the juvenile growth phase. This will be discussed in view of larval development later in the thesis (pp 100-101). Kristensen (1980) also found a similar curvilinear relationship between statolith length and gladius length for gladii less than 50 mm in

length and an approximately linear relationship for larger specimens. It may be noticed that on the graph here presented, specimens of DML between 100 mm and 125 mm represent data points above the regression line, while those between 160 and 190 mm DML yield points below the line, and those of DML exceeding 225 mm again tend to lie above the line. This may be due to a continued growth rate increase for the DML up to about 200 mm, followed by a growth deceleration. It is noteworthy that the specimens occupying the proposed region of decreased growth rate on the graph are also in the R3 stage of development typified by decreased food intake and narrow increments being formed on the statolith. Again, further discussion of these and other biological characteristics concomitant with R3 development are to follow (pp 102-103).

The plotting of the number of increments in the statolith against DML (Fig. 23) shows a large y-intercept at DML = 0. Although the absolute mathematical relationship itself is nonsensical at DML = 0, a consideration of the embryological development sheds some light on the comprehensibility of the problem.

Based on embryological developmental stages of Loligo pealei presented by Arnold (1965) and photographs of developmental stages in embryos of Illex illecebrosus by O'Dor, et al (1982), the statocyst (and presumably the statolith also) forms when the DML is approximately 0.2 mm, or less than one-quarter of the length of the embryo. This yields a y-intercept very near zero. At the time of hatching, the DML is about 1.5 mm (O'Dor et al 1982) which is still very near zero relative to the range of the x-axis. However, as we shall see, the statolith nucleus has now formed at hatching, with averages of 38 increments

formed in females and 43 in males. With a continued slow growth rate of the mantle relative to the statolith in early development, as already shown to be the case, the ratio of the number of increments to the DML would very quickly reach a value compatible with the regression line.

It is noteworthy to observe similar positions on the graph for specimens of DML between 100 and 125 mm and between 160 and 190 mm in Figure 23 as on the graph previously discussed (Fig. 25). This lends further credence to the postulation of an increased growth rate of the mantle up to 200 mm DML.

A comparison between Figures 24 and 26 shows that generally there is less variation in statolith length than in the number of increments of which the statolith is comprised. Consequently, if the hatching date could be determined, the size of the statolith could be of equal or even greater accuracy in determining age than the use of increments counts. The assessment of the time of hatching, as determined in this work, largely depends on the evaluation of the regions of growth of the statolith and the developmental series which now follows.

The kernel of the statolith is analogous to that of fish otoliths in that it represents the formation or growth of the statolith prior to the deposition of clearly recognizible increments. Thus, as previously noted, the statolith exists in the form of a very small kernel before the deposition of increments.

In furthering the analogy, the nucleus of fish otoliths consists of the kernel plus the first opaque ring (Pannella, 1980). Such a prominent ring can be found around the kernel of statoliths of <u>I.</u>

illecebrosus (Figs. 19 and 20) thus enabling the observer to distinguish the kernel from the adjacent R1 area. The argument can be made that the nucleus is, in its entirety, a very small portion of the statolith and not a larger region as some authors have stated.

For example, Rosenberg, Wiborg and Beth (1981) gave a mean measurement of 18 µm with a standard deviation of 4 µm for the area which they designated as the nucleus of statoliths from the ommastrephid Todarodes sagittatus. This value compares closely with my calculated mean measurements of the maximum nuclear radius of 16.9 µm with a standard deviation of 1.5 µm for I. illecebrosus. No other authors refer to such a small nuclear area.

The statolith region herein known as R1 is typified by increments which may vary somewhat in width but have rings which are quite consistent in their darkness. Region one thus has a "homogeneous" appearance relative to R2, where increment width and ring darkness are much more variable.

Several authors publishing on cephalopod statoliths have equated R1 with the nucleus. Discussion of the types of increment arrangements which they describe can be facilitated by reference to Figure 29.

Kristensen (1980) describes the nucleus of G. fabricii as being 160 µm in diameter and labels that area as Zone I. It is clear that this is not to be equated with the true nucleus but rather corresponds structurally to the area which I have designated as R1 in the statolith of I. illecebrosus.

Spratt (1979), working with the loliginid Loligo opalescens, describes an area of increments with uniformly narrow widths in

FIGURE 29. Diagrammatic representations of tracings to show the different patterns of increments in different areas of statoliths as described and labelled by various authors.

A. Spratt (1979) on Loligo opalescens

N - "Nucleus"

E - Extra-nuclear area

B. Kristensen (1980) on Gonatus fabricii

Z1 - Zone One

Z2 - Zone Two

Z3 - Zone Three

Z4 - Zone Four

C. Morris (1983) on Illex illecebrosus

R1 - Region One

R2 - Region Two

R3 - Region Three

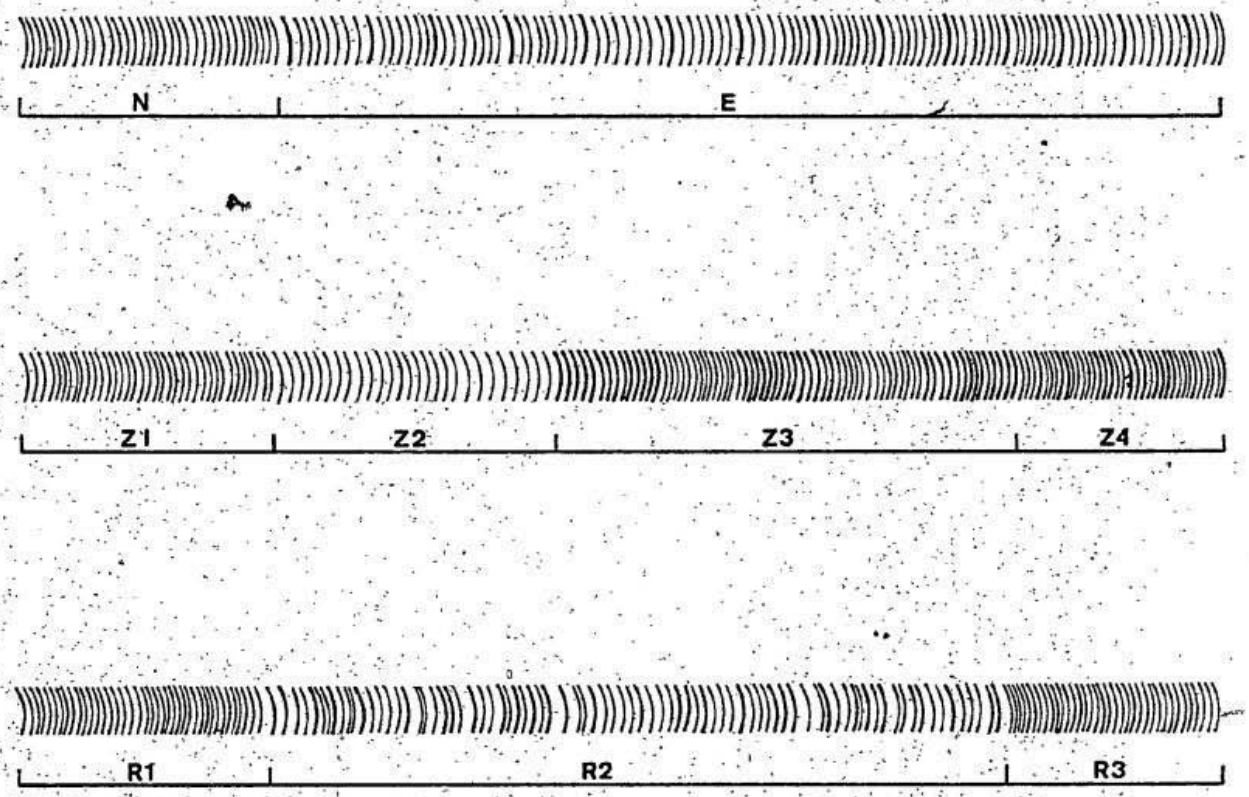
A
N
E
B
Z1
Z2
Z3
Z4
C
R1
R2
R3

"young" specimens and larger increments of irregular thickness separated by five or six smaller increments "in older". The area characterized by narrow, evenly spaced increments is the area he equates with the "nucleus". As in the case reported by Kristensen (1980), Spratt's designation "nucleus" also corresponds to what I have designated as RI, with RI herein being exclusive of the nucleus.

Lipinski (1978) describes the nucleus of the statoliths of I. illecebrosus as having about 40 narrow growth increments. This is undoubtedly RI, not the nucleus. Incidentally, he labels the area of "narrow rings" which make up the structure he calls the nucleus as the "juvenile statolith".

Apparently, these authors (Kristensen, 1980; Spratt, 1979; and Lipinski, 1978) do not recognize the distinction between the kernel-type prototypal nucleus from the adjacent growth area, RI. I see little justification for failing to delineate the nucleus from RI for reasons of striking visibility, clearly indicating its unique nature (Fig. 19), and for reasons evident upon consideration of the ontogeny of the individual statolith. As I have stated, the nucleus represents the statolith in its entirety at a very early stage in the life of the ommastrephid and the development of the statolith. The region designated RI is clearly distinguishable from the nuclear area, as well as from R2, and I cannot, both for morphological, incremental pattern, or biological reasons accept the contention of others that the nucleus represents RI, even in part. Kristensen, Spratt and Lipinski are to be criticized for not realizing that RI is best interpreted as a distinct entity from the nucleus. Hopefully, techniques will be found as this study is continued to unveil any record of nuclear growth which may be locked within the kernel which the nucleus contains.

An insight into the nature of RI can be gained from an examination of Figures 24 and 26. We may note here that the predicted date of initial increment formation (assuming a daily rate) is mid-December whereas the predicted date of initial statolith formation is on or about January 21st. This is obviously an impossible situation but the contradictory predictions may be resolved by the following explanation.

If we assume that RI is completely formed at hatching, as has been shown to be the case for the equivalent region in statoliths from G. fabricii by Kristensen (1980), then the spawning date advances by 38 increments (the number of increments in RI) from mid-December to approximately January 26th. Though this leaves only five days between the first appearance of the statolith and the completion of R1 with 38 increments, it coincides with the approximate time of statocyst formation at about four to five days after fertilization (based on photographs by O'Dor, et al (1982) and embryonic stages of Arnold (1965). It also coincides with hatching at approximately ten days after fertilization. Rapid statolith development can be facilitated by a continuous food supply from the yolk. The consistent optical density of the rings in RI and the relative consistency of increment widths help bear out this hypothesis. Furthermore, extremely rapid rates of increment deposition can be found in other molluscs, such as larval pteropods where averages of 12 increments per day can be placed on the shell (Pannella, 1980).

A further argument that RI must have been formed before hatching is the predatory habit of the rhynchoteuthion. Having little or no remaining yolk at hatching, the larva must rely on prey for sustenance. This implies some degree of manoeuverability and equilibrium detection

which, in turn, implies a statocyst/statolith system of sufficient complexity to accommodate this life style. In the light of the above arguments, it is difficult to refute the presence of R1 of the statolith at the time of hatching. Furthermore, the date which I predict for the completion of R1 formation (January 26th) coincides well with the predicted spawning date of late January or early February (based on regression by mean mantle length) by Squires (1967) and coincides with the capture of rhynchoteuthid and post-rhynchoteuthid larvae of I. illecebrosus in February by Lu and Roper (1979) and Vecchione (1978).

Region two (R2) begins formation upon hatching and at the time of its completion comprises the bulk of the increment-bearing portion of the statolith. It is also this region which is typical of all the stages of statolith development from the end of the primordial stage to the beginning of the adult. Consequently, R2 is the region responsible for the species-characteristic form of the statolith in the adult configuration and is the region which bears the largest and best record of events during the development. The increments of R2 are more variable in width and the rings more variable in darkness than in R1 or R3, indicating that R2 represents the period when the squid is most exposed to environmental variation which causes perturbations in regular increment formation.

The "extranuclear" area described by Spratt (1979) is the area in which he finds rings larger and more irregularly-spaced than those laid down in younger specimens. Because of the contiguity of the "extranuclear" area with the "nucleus" (as designated by Spratt) and the irregular quality of the rings, I equate the extranuclear area of the statolith of L. opalescens with R2 of the statolith of I. illecebrosus.

Lipinski (1978) observed wide growth increments outside RI and ascribed a monthly periodicity to them. However, these monthly increments are obviously not the increments which I describe, since in adult specimens he concluded an age of two years. If I were to assign a monthly periodicity to the increments which I describe, I obtain an adult age of 15 years. This is untenable both because of the evidence of a one or one-and-a-half year life cycle (Mesnil, 1976; Squires 1967) and the heavy predation by pothead whales (Globicephala melaen (Traill)), numerous species of fish and sea birds, and man. Evidently, the preparation methods used by Lipinski in his early study (1978) did not allow the degree of resolution which I and other authors have obtained. However, Lipinski (1980) later revised his estimate to a daily periodicity of increment formation and shows more increments than described in his earlier work.

Kristensen (1980) describes an area which he labels as Zone 2 as being "light and rather uniform". I find no such corresponding area immediately outside RI in I. illecebrosus probably due to some yet unknown differences in the biology of these two species in early larval life. However, he describes Zone 3 as "dark and obviously divided into periodical increments". Based upon this description and the configurations evident in photographs of ground statoliths of G. fabricii, I equate Zone 3 of G. fabricii with R2 of I. illecebrosus.

It is early in the formation of R2 that we observe an increase in the growth rate of the mantle relative to the statolith length.[1] Although this change apparently occurs in a portion of the graph for

---

[1] We note that the change in K is due to an effect on the mantle length and not the statolith length because an effect on the statolith would be reflected in a change in the width or arrangement of the growth increments. No such major perturbation occurs in R2 and the relationship of number of increments to statolith length (Fig. 22) is essentially linear.

which I have no data, we may estimate that this transition occurs at an approximate DML of 50 mm. This size is also the approximate DML which I would expect to correspond to the pre-juvenile stage of statolith development which is characterized by the formation of the basic structures found in the adult statolith.

Furthermore, it may be noted that the largest of the specimens taken in late February and early March with DML of 30 mm still possess characteristics which, according to Nesis (1979), are typical of cephalopod larvae, such as a thin and somewhat saccular mantle, ventral ovoid liver and ink sac, fourth arms which do not yet exceed the lengths of the first arms, a fin which is much smaller relative to the mantle length than in the adult and suckers on more than half the tentacular length.

The above notwithstanding, I have observed that the smallest specimen collected (13.5 mm DML) possessed all of the characteristics outlined above and cited by Nesis as larval characteristics. Indeed, other of these characteristics reminiscent of the rhynchoteuthid morphology were demonstrated by the smallest specimens, including a posteriorly convex fin configuration, sucker buds or primordia on the tips of the arms and a wide proximal aperture to the hyponome.

Because of the above factors and because there is no clear discontinuity in R2 of the statolith which corresponds to the change from the rhynchoteuthid to the post-rhynchoteuthid stages, I do not accept the concept that the larval stage of the Ommastrephidae ends with the division of the rhynchus to form the tentacles, as stated by Roper and Lu (1978). In fact, based on the demarcation of larval phase transitions by changes of growth constants in fishes (Nesis, 1979), the

larval stage of I. illecebrosus extends beyond the end of the rhynchoteuthion at 7.5 to 8.5 mm DML, even to the change in the growth coefficient of the mantle at 50 to 70 mm DML. This change in growth coefficient is accompanied by 1) the development of the statolith into a similar but slightly smaller form than in the adult 2) by the development of the internal organs to their adult configurations (with the gonads as exception) and 3) by the development of the statolith into a similar but somewhat smaller form than found in the adult.

All specimens of I. illecebrosus captured in October and used in this study bore narrow evenly-spaced growth increments on the periphery of the increment-bearing portion of the statoliths. This area of narrow increments is R3.

As previously discussed, the specimens representing the October data appear to exhibit a slight decrease in the rate of growth of the mantle. The main cause of slowed growth in marine invertebrates is decreased food intake (Hallam, 1965) and such deprivation of even fasting can induce narrowing of growth increments in shells of Mercenaria mercenaria (L.) (Pannella and MacClintock, 1968) and in otoliths of the drum fish Lepomis cyanellus Refinesque (Taubert, 1975).

Rowe and Mangold (1975) reported that sexual maturation could be induced in I. illecebrosus by starvation of laboratory-maintained specimens. I have noted voluntary fasting despite food availability in laboratory specimens of this same species during the late inshore season, such fasting being accompanied by sexual maturation, i.e., enlargement of the gonads and other accessory sexual organs such as the nidamental glands, oviducts and others. Similar voluntary food deprivation occurs during sexual maturation in Octopus vulgaris (Wells and Wells, 1977).

All specimens collected in October in this study not only were in the R3 stage of statolith growth, but were also noted to have some degree of gonadal development. Because all the specimens collected in October were in the R3 stage of statolith growth and exhibited gonadal development, it is entirely plausible that R2 represents the phase of growth which prepares the squid morphologically for its optimum fitness and R3 represents the phase of fasting and preparation for spawning.

Despite good reproducibility of increment counts for individual statoliths, increment counts for samples taken at a point in time for single populations have ranges and standard deviations which are too wide to estimate age given small sample sizes. These variations in counts are probably due to differences in the conditions to which individuals were subjected during growth. Food availability, disease, temperature changes and oxygen debt are factors known to affect increment formation in other molluscs such as Mercenaria mercenaria (L.) (Kennish, 1980).

The use of statolith length to determine age may be more useful than increment counts because the variations in statolith length are less than those of increment counts for a given sample. This is, of course, based on the assumption that all the members of a given school of squid are the same age. A uniform age appears to be the case since DML of each sex and statolith length are generally subject to little variation within a sample and bimodal distribution of increment counts within a sample have not been noted.

The use of statolith length to determine age has many advantages over the use of numbers of statolith growth increments for the same purpose. These include: (1) the ranges and standard deviations of

statolith lengths within a given sample are generally much less than the relative ranges and standard deviations obtained for increment counts; (2) intraindividual variation in statolith length is minimal although statolith form and increment counts sometimes vary; (3) observer bias is minimal; (4) interobserver variation is minimal; (5) the only major equipment required is a microscope with a calibrated eyepiece micrometer; (6) very little instruction is required to learn the techniques; (7) the results are highly reproducible for any given specimen; (8) time expenditure is considerably less than that involved in mounting, grinding and repeatedly counting growth increments. These factors lend this method to practical use in fisheries management and private consulting where time and financing may be prime considerations.

The obvious fault in this technique is that it does not include a record of the history of the animal. Such a record is incorporated in the statolith by the increments. The elucidation of environmental effects on increment formation would perhaps allow us to determine why some years are characterized by large numbers of squid in inshore Newfoundland to determine why in other years the squid are very few, and to predict squid abundance. This is especially useful since the success of the Newfoundland inshore fishery is largely based on the availability of squid as bait and prey for commercially sought species.

Both an understanding of increment formation and the development of a more accurate growth curve must rely on more samples being taken at various times during the year and upon larger numbers of specimens in each sample. With the availability of such large numbers of

individual specimens to work with, counting the increments by eye would involve several counters who must be trained. This alone introduces the possibility of error or variation between observers. A more precise and a more economically and temporally efficient method would involve use of an optical microdensitometer attached to a computer link-up. Input signals from the densitometer could be compared to a standardized scale and increments could be automatically counted as totals or subtotals of increments of different densities. Such "counting" could be performed by a single person and thus reduce observer "bias". Use of a standardized scale would eliminate subjective designations of "light" and "dark" increments and, depending on the scale of gradation, lead to the possibility to detect increments not visible by any other method presently used.

The statolith and the surrounding structures of the statocyst are intimately integrated in the proprioception of the spatial orientation and changes in positioning of the cephalopod. We may thus expect any change in the functional form of the statolith to be reflected in statocyst structure and vice versa. However, with the present state of knowledge, we do not know the interrelating factors of statolith and statocyst morphologies even though Clarke (1978), Clarke and Fitch (1980), Clarke, Maddock and Steurbaut (1980), and Dilly (1976) have described several teuthoid statoliths and Ishikawa (1924) has described many cephalopod statocysts.

From the present work herein reported, we see that the statolith rapidly increases in size compared to the mantle length in embryonic and larval specimens. This is further supported by the presence of very large statocysts relative to body size in newly hatched cephalopods

(Ishikawa, 1924; Sacarrao, 1943; Pickford, 1940). Because statocyst/statolith function depends on linear and centripetal forces, statolith and statocyst size variations can be explained by brief reference to the mathematical formulation of centripetal force acting on any particle turning about a point, namely,

$$F = \frac{m v^2}{r}$$

where F = centripetal force

m = mass of the object

v^2 = velocity of the object about a point

r = radius of turn

Suppose we conceive of two structurally identical squids of different lengths executing the same turn relative to their sizes, over the same period of time. We note that the smaller squid turns about a smaller radius and increases the relative force, but the velocity (unit distance per unit time) is also less than in the larger animal. Although the decreased radius causes a mathematically linear increase in force, the accompanying decrease in velocity causes a simultaneous exponential decrease in force. This causes a net loss of centripetal force in the smaller specimen. The maintenance of a force of sufficient amplitude to equal that of the larger animal may be maintained by increasing the mass being acted upon, i.e., the statolymph or the statolith, relative to the size of the total animal. In fact, a statocyst which is large relative to the overall body size has been noted in several larval cephalopods (Ishikawa, 1924; Pickford, 1940; Sacarrao, 1943). Conversely, the statolith of the giant squid <u>Architeuthis dux</u> Steenstrup 1857 is very small compared to the body size of the animal (Morris, 1980).

The use of the techniques herein described can be utilized in an examination of the two size classes so often noted in Conception Bay and other inshore waters of Newfoundland. If sufficient squid were available such that one could take regular samples through an entire inshore season, a season characterized by a bimodal size distribution, then comparison of statolith size and the number of increments therein could elucidate the nature of the bimodality noted.

In that vein, assuming that increments are laid down with regularity, a larger squid containing a statolith with the same number of increments as a smaller one implies faster growth for the larger specimen. Alternately, significantly different increment counts for the two size classes implies that the squid are of different ages. The greatest obstacle with this or any type of population study of I. illecebrosus is finding squid on subsequent occasions in a given season in a particular area to help prevent possible sampling of different stocks. Such unbiased sampling is rarely possible even during years when squid are plentiful and relatively easily available for biological study.

Let us now turn to a discussion of the ontogenetic development of the Illex statolith. The lachrymiform configuration of the Primordial stage of statolith development forms during the period of R1 formation and the lachrymiform shape can be seen by tracing, in any plane parallel to the long axis of the statolith, a single R1 increment along its entire course around the nucleus. The same form can be traced for the earliest increments of R2, but the shape soon becomes distorted as the statolith enters the Definitive stage of development at a size with a DML of approximately 14 mm. Consequently, the Primordial stage is present during the entire rhynchoteuthid larval stage and for part of the post-rhynchoteuthid larva.

It is in the Definitive and Pre-Juvenile stages that the greatest changes in the form of the statolith occur. These stages are found to be representative of specimens in the later larval stages, i.e., the post-rhynchoteuthion, and characterize morphological alterations in the configuration of the statolith from the lachrymiform one of the Primordial to the more complex shape seen in the Juvenile stage.

The anlagen, or foundations, of specific statolith structures so clearly evident in the Adult stage arise during the Definitive stage. The single exception to this is the rostrum anlage, which is first evident in the Primordial stage, assuming a configuration clearly similar to the adult rostrum as early as the Definitive stage.

During the Pre-Juvenile stage, the anlagen are developed to such an extent that the statolith is characterized by all the adult structures in their proper positions and in approximate proportions. It is of importance to note here that the end of the Pre-Juvenile stage roughly corresponds to the change in growth constant (DML/statolith length, Fig. 25) of the development of the mantle which signals the end of the larval condition and the first attainment of an adult morphology, albeit in miniature.

During the Juvenile stage of development, the Adult statolith form is clearly discernable and, with the exception of the sexual organs, the body morphology is essentially that of the adult. This stage is therefore not one particularly characterized by a change in statolith shape, but of an increase in size of the statolith, even to the size characteristic of the adult form.

A clear demarcation between Juvenile and Adult statolith forms is difficult to define, but it may be said that the ventral portion of the

medial fissure is widely open in the Juvenile stage and closing in the Adult, and the foramen of the Juvenile shows no deposition of crystals.

The Advanced stage is very uncommon, having been found in less than 1% of the more than 400 pairs of statoliths of I. illecebrosus I have examined. Although specimens with the foramina filled are often found, an accompanying closure of the medial fissure is very atypical, particularly closed to the extent as is illustrated in the specimen shown in Figure 18. This form, i.e., the Advanced stage, may conceivably be within the range of normal variation that may be expected in the adult configuration, but at the present time I have no basis for an explanation of this phenomenon, other than to suggest that it represents the final configuration of the statolith that is typical of the Ommastrephid after it has left the insular waters of Newfoundland and begun its supposed southerly migration and its assumption of its basic oceanic habit.

Future study must be undertaken in which more specimens representing forms from a wider range of distribution, size and age will be incorporated. To understand the physiology of this species with particular reference to the functional morphology of the statocyst/statolith system of maculae, cristae, and "stone", studies must not deal exclusively with the configuration of, and changes in, the statolith, but be concerted with studies of its interactions with the maculae and the cristae, i.e., the entire statocyst complex.

Little is known of the interrelations of statolith and statocyst forms, of how these forms are determined, or even how the different morphologies of these highly sophisticated balance organs are adapted to the mode of life of the forms containing them. It is clear that a full

understanding of the statocyst/statolith system depends on how and why each portion of the system grows and attains its functionally optimal configuration in each species.

CONCLUSIONS

(1) The repeating patterns of light and dark lamellae in statoliths of *Illex illecebrosus* are true growth increments.

(2) A suitable mounting and grinding method with a high success rate has been developed for the preparation of teuthoid statoliths from both sexes to allow viewing of the increments therein contained.

(3) The simple tracing method of recording such increments has numerous advantages over previously described methods and is easily adapted for examination of fish saggitae.

(4) Age of specimens of *I. illecebrosus* may be more accurately determined by statolith length than ~~by~~ statolith increment counts up to approximately six months of age.

(5) The statolith increases in size very rapidly during the embryonic growth phase. This period of statolith growth is demarcated by the primordial stage of statolith growth and type of increments.

(6) Postembryonic growth to the onset of gonadal development and sexual maturity is represented in the statolith by a region of growth increments characterized by highly variable increment width and ring opacity.

(7) As sexual maturity approaches, the increments on the statolith become more narrow and more uniform in their width.

(8) The larval stages of the development of *I. illecebrosus* extend well past the end of the rhynchoteuthion stage at 7.5 to 8.5 mm DML, up to 50 to 70 mm DML when the squid resembles a miniature adult.

(9) The form of the statolith changes radically during larval development until it approaches a shape approximating that of the adult. This shape is formed during the pre-juvenile stage which heralds the end of larval development.

REFERENCES CITED

ARNOLD, J. M. 1965. Normal Embryonic Stages of the Squid Loligo pealei (Lesueur). Biol. Bull. 128 (1): 24-32.

BARBER, V. C. 1965. Preliminary Observations on the Fine Structure of the Octopus Statocyst. Journal de Microscopie, 4:547-550.

_____. 1966a. The Fine Structure of the Statocyst of Octopus vulgaris. Z. Zellforsch. mikrosk. Anat., 70: 91-107.

1966b. The Morphological Polarization of Kinocilia in the Octopus statocyst. J. Anat., London, 100: 685-686.

_____. 1966 a. The Fine Structure of the Statocyst of Octopus vulgaris. Z. Zellforsch. mikrosk. Anat., 70: 91-107.

_____. 1968. The Structure of Mollusc Statocysts, with Particular Reference to Cephalopods. Symp. Zool. Soc. Lond., 23: 37-62.

BURCH, B. L. 1980. Cephalopod Statoliths. Display presented at the 49th Annual Meeting of the American Malacological Union, Louisville, Kentucky, U.S.A., 1980

BUDDENBROCK, W. von, 1915. Die Statocysts von Pecten, Histologie und Physiologie. Zool. Jahrb. (allg. Zool.), 35: 301-356.

BUDELMANN, B. U. 1970. Die Arbeitsweise der Statolithenorgane von Octopus vulgaris. Z. vergl. Physiologie, 70: 278-312.

_____. 1975. Gravity Receptor Function in Cephalopods with Particular Reference to Sepia officinalis. Fortsch. Zool. 23: 84-96.

_____. 1976. Equilibrium Receptor Systems in Molluscs. In: P.J.Mill (Ed.), Structure and Function of Proprioceptors in the Invertebrates. Chapman and Hall, London. pp. 529-566.

_____. 1977. Structure and Function of the Angular Acceleration Receptor Systems in the Statocysts of Cephalopods. Symp. Zool. Soc. London., 38: 309-324.

_____. 1978. The Function of the Equilibrium Receptor Systems of Cephalopods. Proc. Neurootol. Equilibriom. Soc. Vol. VI(1): 15-63.

_____. 1979. Hair Cell Polarization in the Gravity Receptor Systems of the Cephalopods Sepia officinalis and Loligo vulgaris. Brain Res. 160: 261-270.

CHOE, S. 1963. Daily Age Markings on the Shell of Cuttlefishes, Nature, 197: 306-307.

CHUN, C. 1915. The Cephalopoda. Scientific Results of the German Deepsea Expedition on Board the Steamship VALDAVIA 1898-1899. 18: 1-552.

CLARKE, M. R. 1965. "Growth Rings" in the Beaks of the Squid Moroteuthis ingens (Oegopsida: Onychoteuthidae). Malacologia, 3 (2): 287-307.

_____. 1966. A Review of the Systematics and Ecology of Oceanic Squids. Adv. Mar. Biol 4:91-300.

_____. 1978. The Cephalopod Statolith - An Introduction to its Form. J. Mar. Biol. Ass. U.K., 58: 701-712.

_____ and J. E. FITCH. 1975. First Fossil Record of Cephalopod Statoliths. Nature, 257: 380-381.

_____ and _____. 1979. Statoliths of Cenozoic Teuthoid Cephalopods from North America. Palaeontology, 22 (2): 479-511.

_____ and G. E. MAUL. 1962. A Description of the "Scaled" Squid Lepidoteuthis grimaldii Joubin 1895. Proc. Zool. Soc. London, 139 97-118.

_____. L. MADDOCK and E. STEURBAUT. 1980. First Fossil Cephalopod to be Described from Europe. Nature, 287: 628-630.

DAWE, E. 1981 Overview of Present Progress Toward Aging Short-Finned Squid (Illex illecebrosus) Using Statoliths. J. Shellfish Res. 1: 193-195.

DILLON, J. F. and G. R. CLARK, 1980. Growth-Line Analysis as a Test for Contemporaneity in Populations. In: Rhoads, D.C. and R. A. Lutz, Skeletal Growth of Aquatic Organisms. Plenum Press, N.Y., 1980.pp. 395-416.

DILLY, P. N. 1976. The Structure of Some Cephalopod Statoliths. Cell Tiss. Res., 175: 147-163.

EVANS, J. W. 1972. Tidal Growth Increments in the Cockle Clinocardium nuttalli. Science, 176: 416-417.

GORDON, J. and M. R. CARRIKER. 1978. Growth Lines in a Bivalve Mollusc: Subdaily Patterns and Dissolution of the Shell. Science, 202: 519-521.

GRIFFIN, L. E. 1897. Notes on the Anatomy of Nautilus pompilius. Zool. Bull. 1: 147-161.

HALLAM, A. 1965. Environmental Causes of Stunting in Living and Fossil Marine Benthonic Invertebrates. Palaeontology, 8: 132-155.

HAMLYN-HARRIS, R. 1903. Die Statocysten der Cephalopoden. Zool. Jahrb. Abt. Morph., 18: 327-358.

HUMASON, G. L. 1972. Animal Tissue Techniques. W. H. Freeman & Co., San Francisco, U.S.A., 641pp.

HURLEY, G. V. and P. BECK. 1980. The Observation of Growth Rings in Statoliths from the Ommastrephid Squid Illex Illecebrosus. NAFO SCR Doc. 80/II/I, no. 27.

_____, _____, J. DREW and R. L. RADTKE. 1979. A Preliminary Report on Validating Age Readings from Statoliths of the Short Finned Squid (Illex Illecebrosus). ICNAF Re. Doc. 79/II/26.

ISGROVE, A. 1909. Eledone. Liverpool Marine Biology Committee Memoirs, Vol. 18. Williams and Norgate, London, 105 pp.

ISHIKAWA, M. 1924. On the Phylogenetic Position of the Cephalopod Genera of Japan Based on the Structure of Statocysts. J. Coll. Agric., 7 (3): 165-219.

JONES, W. C. 1955. Crystalline Properties of Spicules of Leucosolenia complicata. Q.J. Microscop. Sci., 96 (2): 129-149.

KAHN, P. G. K. and S. M. POMPEA. 1978. Nautiloid Growth Rhythms and Dynamical Evolution of the Earth-Moon System. Nature, 275: 606-611.

KENNISH, M. J. 1980. Shell Microgrowth Analysis: Mercenaria mercenaria as a Type Example for Research in Population Dynamics. In: Rhoads, D.C. and R.A.Lutz, 1980, Skeletal Growth of Aquatic Organisms. Plenum Press, N.Y., U.S.A., pp. 255-294.

KLEIN, K. 1931. Die Nervenendigungen in der Statocyste von Sepia. Zeitschr. Zellforsch. Mikroskop. Anat., 14: 481-516.

KRISTENSEN, T.K. 1980. Periodical Growth Rings in Cephalopod Statoliths. Dana, 1: 39-51.

LIPINSKI, M. 1978. The age of Squids, Illex Illecebrosus (LeSueur, 1821), from their Statoliths. ICNAF Res. Doc. 78/II/15.

_____. 1979. The Information Concerning Research upon Ageing Proceedure of Squids. ICNAF W.P., 79/II/40 (unpublished), (quoted in Lipinski, 1980).

_____. 1980. Statoliths as a Possible Tool for Squid Age Determination. NAFO SCR Doc. 80/II/22.

LU, C. C. 1968. Determination of Growth and Related Phenomena in Illex illecebrosus illecebrosus (Lesueur) (Decapoda: Cephalopoda) from Newfoundland. M.Sc. Thesis, Memorial University of Newfoundland, St. John's, Nfld., Canada. 178 pp.

_____ and C. F. E. ROPER. 1979. Cephalopods from Deepwater Dumpsite 106 (Western Atlantic): Vertical Distribution and Seasonal Abundance. Smithsonian Contributions to Biology, No. 288, Smithsonian Institution Press, Wash., D.C., U.S.A..

MACDONALD, J. D. 1855. On the Anatomy of Nautilus umbilicatus Compared with that of Nautilus pompilius. Philosophical Transactions of the Royal Society of London, 145: 277-288.

MESNIL, B. 1976. Growth and Life Cycle of Squid, Loligo pealei, and Illex illecebrosus from the Northwest Atlantic. Ann. Meeting Int. Comm. Northw. Atl. Fish. Res. Doc 76/VI/65.

METHVEN, D.A. 1983. M.Sc. Thesis (in preparation). Memorial University of Newfoundland, St. John's, Nfld., Canada.

MINA, M. V. 1968. A Note on a Problem in the Visual Qualitative Evaluation of Otolith Zones. J. Cons. perm. int. Explor. Mer 32(1): 93-97.

MORRIS, C. C. 1980. Studies of the Statoliths of the Squid *Illex illecebrosus* (Lesueur, 1821) and *Architeuthis dux* Steenstrup, 1857 with Speculation on their Functional Morphology. B.Sc. (Hons.) Thesis, Memorial University of Newfoundland, St. John's, Nfld., Canada.

____. 1981. Comparative Morphology of Statoliths of Two Squid Species (Abstract). Bull. Amer. Malacol. Union. 1981, p.36.

NESIS, K. K. 1979. Larvae of Cephalopods. Biologiya Morya, 4: 26-37. (Translation in Embryology, 1980, pp. 267-275.)

NIXON, M. 1973. Beak and Radula Growth in *Octopus vulgaris* J. Zool. London, 170: 451-462.

O'DOR, R. K., N. BALCH, E. A. FOY, R. W. M. HIRTLE and D. A. JOHNSON. 1982. Embryonic Development of the Squid *Illex illecebrosus* and Effect of Temperature on Development Rates. J. Northw. Atl. Fish. Sci., 3: 41-45.

OLIVE, P. J. W. 1980. Growth Lines in Polychaete Jaws (Teeth). In: Rhoads, D.C. and R.A.Lutz, Skeletal Growth of Aquatic Organisms, Plenum Press, N.Y., 1980, pp. 561-594.

OWSJANNIKOV, P. and A. KOWALEVSKY. 1867. Uber des Centralnervensystem und das Gehororgan der Cephalopoden. Mem. Acad. Imp. des Sci. de St. Petersbourg, Serie VII, II(3): 1-36.

PANNELLA, G. 1980. Growth Patterns in Fish Sagittae. In: Rhoads, D. C. and R. A. Lutz, Skeletal Growth of Squatic Organisms, Plen Press, N.Y., 1980, pp. 519-560.

PANNELLA, G. and C. MACCLINTOCK. 1968. Biological and Environmental Rhythms Reflected in Molluscan Shell Growth. Quoted in Kennish (1980).

PICKFORD, G. E. 1940. The Vampyromorpha, Living Fossil Cephalopoda. Trans. N.Y. Acad. Sci., Series II, 2: 169-181.

PORTMANN, A. 1960. Generalities sur les mollusques. In: Grasse, P. P., Traite de Zoologie. Masson edit. Paris.

RADTKE, R. L. 1981. The Chemical and Structural Characteristics of Squid Statoliths. Amer. Zool., 21(4): 946.

RHOADS, D. C. and R. A. LUTZ. 1980. Skeletal Growth of Aquatic Organisms. Plenum Press, N.Y., 749 pp. (pp. 1-22).

RICHARD, A. 1969. The Part Played by Temperature in the Rhythm of Formation of Markings on the Cuttlefish (Sepia officinalis L.) (Cephalopoda, Mollusca). Experimentia, 25: 1051-1052.

RICKER, W. E. 1975. Computation and Interpretation of Biological Statistics of Fish Populations. Bull. Fish. Res. Bd. Can., no. 191, 382 pp.

ROPER, C. F. B. and C. C. LU. 1978. Rhynchoteuthion larvae of Ommastrephid Squids of the Western North Atlantic, with the First Descriptions of Larvae and Juveniles of Illex illecebrosus. In: Balch, N, T. Amaratunga and R. K. O'Dor, Proceedings of the Workshop on Illex illecebrosus. Fish. and Mar. Tech. Rept. No. 833, Canada.

ROSENBERG, A. A. 1982. Growth of Juvenile English Sole, Parophrys vetulus in Estuarine and Open Coastal Nursery Grounds. Fish. Bull., 80(2): 245-252.

_____, WIBORG, K. F. and I. M. BECH. 1981 Growth of Todarodes sagittatus (Lamarck) (Cephalopoda, Ommastrephidae) from the Northeast Atlantic, Based on Counts of Statolith Growth Rings. Sarsia, 66(1): 53-57.

ROWE, V. L. and K. MANGOLD. 1975. The Effect of Starvation on Sexual Maturation in Illex illecebrosus (Lesueur) (Cephalopoda: Teuthoidea). J. Exp. Mar. Biol. Ecol. 17: 157-163.

SACARRAO, G. F. 1943. Observations sur les Dernieres Phases de la Vie Embryonnaire de L'"Eledone". Arquivos do Museu Bocage, Lisboa. XIV: 25-35.

SPRATT, J. D. 1979. Age and Growth of the Market Squid, Loligo opalescens Berry, in Monterey Bay. California Dept. of Fish and Game, Fish Bull. 169: 35-44.

SQUIRES, H. J. 1957. Squid, Illex illecebrosus (Lesueur) in the Newfoundland Fishing Area. J. Fish. Res. Bd. Canada 14(5): 693-728.

_____. 1967. Growth and Hypothetical Age of the Newfoundland Bait Squid Illex illecebrosus illecebrosus. J. Fish. Res. Bd. Canada, 24(6): 1209-1217.

STEPHENS, P. R. and J. Z. YOUNG. 1978. Semicircular Canals in Squids. Nature, 271: 444-445.

_____ and _____. 1982. The Statocyst of the Squid Loligo. Jour. Zool. London, 197: 241-266.

TAUBERT, B. D. 1975. Daily Growth Rings in the Otoliths of Lepomis sp. and Tilapia mossambica (Peters). 37th Midwest Fish & Wildlife Conference, Abstracts. (Quoted in Pannella (1980)).

THOMPSETT, D. H. 1939. Sepia. Liverpool Mar. Biol. Comm. Vol. 32, University Press of Liverpool, 184 pp.

TSCHACHOTIN, S. 1908. Die Statocyste der Heteropoden. Z. Wiss. Zool. 90 343-422. (Quoted in Barber, 1968)

VECCHIONE, M. 1978. Larval Illex (Cephalopoda, Oegopsida) from the Middle Atlantic Bight. In: Balch N, T. Amaratunga and R.K. O'Dor 1978, Proceedings of the Workshop on Illex Illecebrosus. Fish. Mar. Ser. Tech. Rep. No. 833.

WELLS, M. J. and J. WELLS. 1977. Optic Glands and the Endocrinology of Reproduction. In: The Biology of Cephalopods. Zool. Soc. London Symposia, 38: 525-540.

YAGI. T. 1960. Bull. Jap. Soc. Sci. Fish., 26: 646 (in Japanese). (Quoted from Choe (1963)).

YOUNG, J. Z. 1960. The Statocysts of Octopus vulgaris. Proc. Roy. Soc. London, (B), 152: 3-29.

_____. 1965. The Central Nervous System of Nautilus. Phil. Trans. Roy. Soc. London, (B): 249: 1-25.

ZAR, J. H. 1974. Biostatistical Analysis. Prentice Hall, Englewood Cliffs, N.J., U.S.A., 620 pp.